

Interacting opinion and disease dynamics in multiplex networks: discontinuous phase transition and non-monotonic consensus times

Fátima Velásquez Rojas and Federico Vazquez

IFLYSIB, Instituto de Física de Líquidos y Sistemas

Biológicos (UNLP-CONICET), 1900 La Plata, Argentina

(Dated: May 25, 2022)

Abstract

We study the dynamics of disease spreading intertwined with that of opinion formation, in a population of agents that interact via two types of links –contact and social–. These two interacting dynamical processes take place on two layers of networks, coupled through a fraction q of links present in both networks. Agents are endowed with an opinion and a disease state that follow the voter and the contact process dynamics, respectively. The update probability of a given state depends on both, the opinion and disease states of the interacting partner: agents are less likely to interact and adopt the opinion of an infected neighbor, while infections are most likely to be transmitted between same-opinion neighbors. We find that healthy-endemic transition observed in the contact process on isolated networks becomes discontinuous in the two-layer system, where the discontinuity jump increases with the coupling q . An abrupt transition is also found as the coupling increases beyond a threshold value q_c . We show that these transitions are discontinuous as long as the networks are finite, while they become continuous in infinite large systems. Furthermore, the dynamics of disease spreading delays the opinion consensus, which varies non-monotonically with q in a large range of the model’s parameters. We present a pair approximation that qualitatively agrees with numerical results, and gives an insight into how the two dynamics affect each other.

I. INTRODUCTION

The set of multiple interactions that characterize social, technological and biological systems are well described by complex networks [1]. In many cases, these networks are interrelated with one another, as they are made up by the same units or nodes, but connected by a different kind of link in each network. For instance, the neural network of the *C.elegans* nematode is composed by 281 neurons that can be connected either by a chemical link or by a ionic channel; and each type of connection has a completely different dynamics [2]. This intertwined networked system can be represented by a multiplex network [2–4] of 281 nodes and two layers of interacting networks; one formed by chemical links and the other by gap junctions’ interactions, each supporting a different process. Another example is given by the network of physical contacts –formed by people having daily face-to-face contacts–, which interacts with the network of social relations –formed by individuals that influence each other on a social issue–. Individuals are the same in both networks and can be connected by two types of links –contact and social–. For instance, two close friends can have both, a contact and social tie, as they can see each other at work every day and also interchange ideas on a political issue. But it can also happen that individuals are connected by only one type of tie; e.g., two colleagues having a contact or proximity relation because they work in the same place but never talk about politics; or two friends that never meet but discuss political ideas by electronic means (phone, Facebook, Twitter, email, etc).

The type of dynamical processes that can take place on each network are very different in nature. It is known that some contagious viral infections like flu are transmitted by proximity or direct contact between individuals, causing a propagation of the disease on the contact network; while social networks can support processes that involve peer pressure, like the adoption of new behaviors or opinions, among others. In this article we study how disease spreading and opinion formation processes affect each other within the multiplex framework, i.e., when actors are the same in both layers of networks but connections may be different. We implement two simple models as a proxy of each process, the contact process (CP) and the voter model (VM). The CP has been extensively studied to explore the spread of an infection in a system of interacting agents or particles [5], where infected agents can transmit the infection to susceptible neighbors in a lattice [6] or a complex network [7], and they can also recover at a given rate. The VM, on its part, was originally introduced as the

simplest system of interacting particles that can be exactly solvable in any dimension [8–10], and is one of the most studied models for opinion consensus. In this model, individuals can take one of two possible positions or opinions on a given issue –like to be either in favor or against marijuana legalization–, and are allowed to update them by adopting the opinion of a randomly chosen neighbor.

Some related works on multilayer networks [11–16] explored the interrelation between two information spreading processes that are alike, but specific studies on the interplay between the dynamics of opinions and diseases are less known. In references [11, 12], the authors analyzed how the awareness of a disease affects the epidemic spreading on a multiplex network, by using the unaware-aware-unaware and the susceptible-infected-susceptible cyclic models, respectively. The interplay between opinion formation and decision making processes was studied in [13] using two interconnected networks. Another work considered two political parties (two interacting networks) that compete for votes in a political election [14]. In a recent article [15], the authors studied the dynamics of the voter model on bilayer networks with coevolving connections, while in [16] the same authors explored whether is appropriate to reduce the dynamics of the voter model from a two-layer multiplex network to a single layer.

In this article we show that the healthy-endemic phase transition in the CP changes from continuous to discontinuous when the disease and opinion dynamics are coupled, and that the diffusion of opinions is slowed down by the disease in a non-trivial manner, leading to consensus times that vary non-monotonically with the coupling. Changes in the order of topological and dynamical transitions were already observed in multilayer networks [17–23]. For instance, a recent work [24] considers a complex threshold dynamics that competes with a simple Susceptible-Infected-Susceptible dynamics (SIS) on two interconnected networks. They find that the discontinuous (continuous) transition observed in the threshold (SIS) model on isolated networks can become continuous (discontinuous) depending on the relation between the intra and internetwork connectivities.

The article is organized as follows. In section II, we introduce the multiplex framework and the dynamics of the model on each layer. We present simulations results in section III and develop an analytical approach in section IV. Finally, in section V we give a summary and conclusions.

II. THE MODEL

We consider a bilayer system composed by a contact and a social network layer of mean degree $\langle k \rangle = \mu$ and N nodes each. These two layers are interrelated through their nodes, which are the same in both networks, while links connecting nodes may not necessarily be the same. That is, both layers have the same number of nodes N and links $\mu N/2$, but the configuration of connections can be different in each layer. The overlap of links is measured by the fraction q ($0 \leq q \leq 1$) of links shared by both networks. The extreme values $q = 0$ and $q = 1$ correspond to totally uncoupled and totally coupled networks, respectively. To build this particular topology, we start by connecting the same pairs of nodes at random in both networks until the number of links reaches the overlap value $q\mu N/2$. Then, the rest of the links $(1 - q)\mu N/2$ are randomly placed between nodes in each network separately, making sure that the chosen pair of nodes in one network is not already linked in the other network.

Social links in this system connect individuals that influence each other on a given issue, while the infection is transmitted through contact links. In Fig. 1 we illustrate the bilayer system composed by a social and a contact network (top and middle layers), and its representation as a single layer with two types of links (bottom layer). We observe in Fig. 1 that nodes i and j are connected by both a social and a contact link, representing individuals that have a daily face-to-face (F2F) conversation, where they interchange opinions and also one can infect its partner. Nodes j and k are only connected by a social link: they do not have F2F contacts but still exchange ideas electronically or by phone. And nodes i and k are only connected by a contact link: they have F2F or proximity contacts but they do not discuss and interchange opinions about the given issue.

To mimic the spreading of opinions and the disease we use the voter model (VM) and the contact process (CP) on each layer, respectively. Each node is endowed with an opinion state \mathcal{O} that can take two possible values $\mathcal{O} = +, -$ (see top layer of Fig. 1), and a disease state $\mathcal{D} = 0, 1$ that represents the susceptible and infected states of an individual, respectively (middle layer of Fig. 1). These two dynamics are coupled through the states of the nodes, which affect each other. On the one hand, we assume that individuals are less influenced by sick partners, because daily contacts are normally reduced in that situation. On the other hand, we consider that disease spreading is more likely to happen between same-opinion

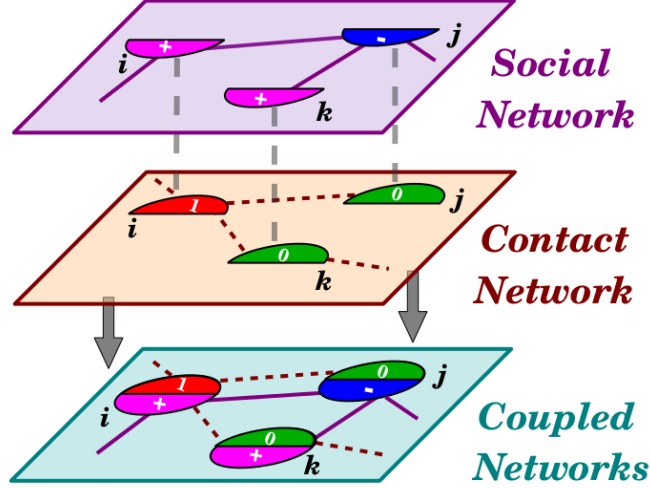


FIG. 1: Schematic diagram showing a small part of a two-layer multiplex network. The top layer represents a social network supporting the propagation of opinions, while the middle layer describes a network of physical contacts on which a disease spreads. The bottom layer is the collapse of both layers, showing nodes connected by social (solid lines) and contact (dashed lines) links. Node states are susceptible (1) and infected (0) in the contact network, and follow the contact process dynamics, while + and - states in the social network are updated according to the voter model dynamics.

individuals, as homophily tend to make relations more frequent and longer.

In a single time step $\Delta t = 1/N$ of the dynamics, an opinion and a disease update attempt take place in each network, as we describe below (see Fig. 2).

Opinion Update [Fig. 2(a)]: a node i with opinion \mathcal{O}_i and one of its neighbors j with opinion \mathcal{O}_j are randomly chosen from the social network. If $\mathcal{O}_i = \mathcal{O}_j$ nothing happens. If $\mathcal{O}_i \neq \mathcal{O}_j$, then i copies the opinion of j ($\mathcal{O}_i \rightarrow \mathcal{O}_i = \mathcal{O}_j$) with probability p_o if there is a contact link between i and j , and at least one of the two nodes is infected ($\mathcal{D}_i = 1$ or $\mathcal{D}_j = 1$). Otherwise, i.e., if there is no contact link or $\mathcal{D}_i = \mathcal{D}_j = 0$, then i copies j 's opinion with probability 1.0.

Disease update [Fig. 2(b)]: a node i with disease state \mathcal{D}_i is chosen at random from the contact network. If $\mathcal{D}_i = 0$ nothing happens. If $\mathcal{D}_i = 1$, then i recovers with probability $1 - \beta$ or, with the complementary probability β node i tries to infect a randomly chosen neighbor j , as long as it is in the susceptible state ($\mathcal{D}_j = 0$). The infection happens ($\mathcal{D}_j = 0 \rightarrow \mathcal{D}_j = 1$)

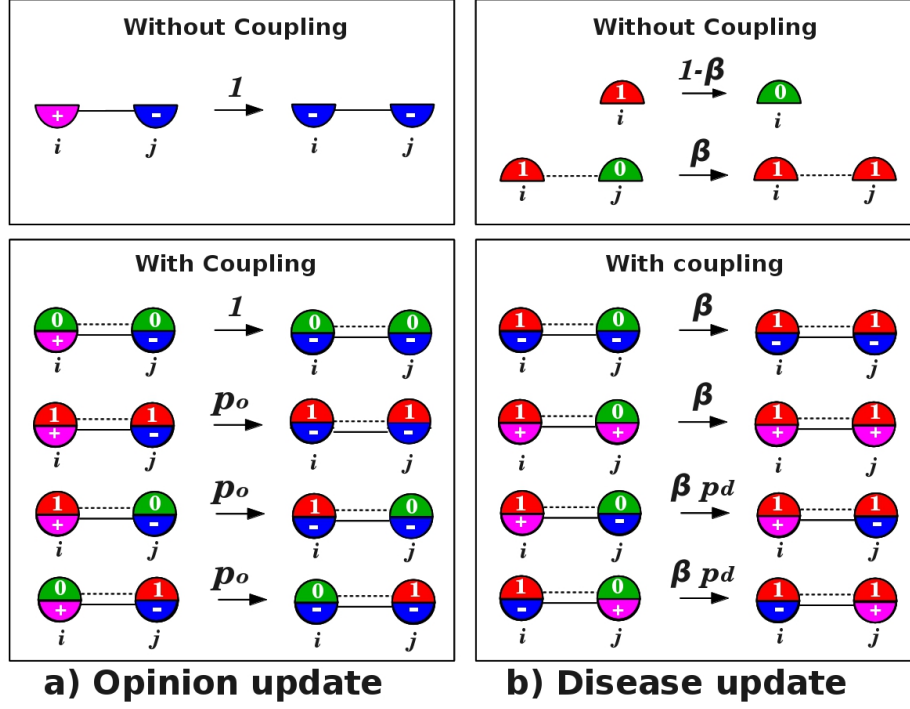


FIG. 2: Update rules in the coupled opinion-disease system. (a) Opinion update. Node i adopts the opinion of its neighbor j with probability 1.0 when they are connected only by a social link (solid line). When they are also connected by a contact link (dashed line), adoption happens with probability 1.0 if both nodes are susceptible, and with probability $p_o \leq 1.0$ if at least one node is infected. (b) Disease update. An infected node i recovers with probability $1 - \beta$ or transmits the disease to a susceptible neighbor j with probability β when both nodes are only connected by a contact link, or when they are connected by both types of links and they share the same opinion. In case they hold opposite opinions the transmission happens with probability $\beta p_d \leq \beta$.

with probability p_d if there is a social link between i and j , and $\mathcal{O}_i \neq \mathcal{O}_j$. Otherwise, i.e., if there is no social link or $\mathcal{O}_i = \mathcal{O}_j$, then node j is infected with probability 1.0.

In other words, individuals on the social layer adopt the opinion of their neighbors with probability 1.0 except when they are connected by a contact link and one of them is infected, where in this case the opinion is adopted with a reduced probability $p_o \leq 1$ [see Fig. 2(a)]. The CP dynamics spreads on the disease layer with an infection probability β between two neighbors, which is reduced to $\beta p_d \leq \beta$ only in the case they are attached by a social link and they share different opinions [see Fig. 2(b)].

This particular dynamics tries to mimic a possible scenario where opinions and disease affect each other, by reducing the flow of information between neighbors. On the one hand, sick individuals usually stay at home or at hospitals, reducing contacts with other partners and, consequently, making less likely the interchange of opinions with them. On the other hand, there is a tendency to have a relationship with opposite-opinion individuals that is less frequent than that with same-opinion peers, thus decreasing the chances to catch a disease from infected partners that hold the opposite opinion.

III. NUMERICAL RESULTS

The CP and the VM are two of the most studied dynamical processes [10]. A relevant feature of the CP is the existence of a transition from a healthy phase to an endemic phase as the infection probability overcomes a threshold value β_c . The healthy phase is static, as all nodes are susceptible and infection events cannot occur. The endemic phase is active, where each node undergoes an infected-susceptible-infected cycle and the total number of infected nodes fluctuates around a stationary value. The healthy-endemic transition is continuous, and the critical value β_c depends on the topological properties of the network [7]. For its part, the VM has been extensively used to explore opinion consensus on different network topologies [25–30]. It was found that the diffusion properties of opinions depend on the heterogeneity of the network. This is reflected in the mean consensus time, which is proportional to the ratio μ^2/μ_2 [29, 30], where μ and μ_2 are the first and second moments of the network’s degree distribution.

The behavior described above is particular of each model on single isolated networks. In order to explore how the properties of these two processes are affected when they are coupled through a multiplex network, we run extensive Monte Carlo (MC) simulations of the model described in section II, using two Erdős-Rényi (ER) networks of mean degree $\langle k \rangle = \mu = 10$ each. Initially, each node in the system is infected with probability 1/2, and adopts either opinion state + or – with equal probability 1/2. That is, the system starts from a symmetric initial condition with roughly 1/4 of nodes in each of the four possible opinion-infection states: $\begin{bmatrix} + \\ 0 \end{bmatrix}$, $\begin{bmatrix} + \\ 1 \end{bmatrix}$, $\begin{bmatrix} - \\ 0 \end{bmatrix}$ and $\begin{bmatrix} - \\ 1 \end{bmatrix}$.

In the next two subsections we study separately the effects of one dynamics over the other.

A. Effects of opinion formation on disease prevalence

We start the analysis of the model by describing the results on the effects of opinion formation on the properties of disease spreading. In Fig. 3 we show the stationary fraction of infected nodes averaged over many independent realizations of the dynamics, $\langle \rho_1^{\text{stat}} \rangle$, as a function of the infection probability β . For this first set of simulations we used $p_o = p_d = 0$, which corresponds to the extreme case scenario where opinions cannot be transmitted across contact neighbors (nodes connected by a contact link) that are infected, and infections are not allowed between social neighbors (nodes connected by a social link) with different opinions. Each curve corresponds to a different value of the coupling parameter q . We observe that, for $q = 0.4$ and 0.7 , $\langle \rho_1^{\text{stat}} \rangle$ decreases smoothly with β until a point β_q^c that depends on q , where it decays abruptly to a value close to zero, showing a behavior that is reminiscent of a discontinuous transition. We also see that the jump in $\langle \rho_1^{\text{stat}} \rangle$ decreases with q and vanishes for the uncoupled case $q = 0$, where the transition becomes continuous, in agreement with the known behavior of the CP on isolated networks. The critical point $\beta_0^c \simeq 0.53$ for $q = 0$ agrees very well with the one found in previous numerical and analytical works [7]. We have checked that the stationary value ρ_1^{stat} is independent on the initial condition (not shown), by running simulations starting from a configuration where a random node and its neighbors are infected (infectious seed), and opinions are distributed as described above.

These results show that the dynamics of opinions has a profound effect on the statistical properties of disease spreading, changing the type of phase transition in the CP from a continuous transition in the absence of coupling (when the two dynamics are independent) to a discontinuous transition when the dynamics are coupled. In real populations, the implications of having continuous in contrast to discontinuous transitions are very different. Indeed, starting from a hypothetical situation that consists on a population of individuals with an infection rate just below the critical value (in the healthy phase), a small increment in β would lead to a small number of infected individuals in the former case, but a large number of infections in the later case. Therefore, disregarding the effects of social dynamics on epidemics propagation could lead to an underestimation of the real magnitude of the spreading.

In order to achieve a deeper understanding of the nature of this transition we studied the time evolution of the fraction of infected nodes $\rho_1(t)$ for the case $q = 0.4$, where the transition

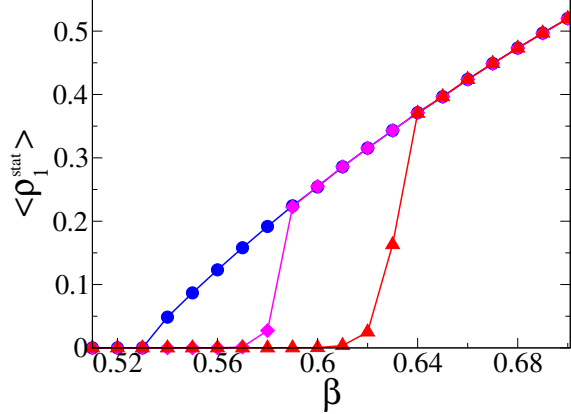


FIG. 3: Average stationary density of infected nodes $\langle \rho_1^{\text{stat}} \rangle$ vs infection probability β on two coupled ER networks of mean degree $\mu = 10$ and $N = 10^4$ nodes each, for $p_o = p_d = 0$ and coupling parameters $q = 0$ (circles), $q = 0.4$ (diamonds) and $q = 0.7$ (triangles). The average was done over 5000 independent realizations starting from configurations consisting on a fraction close to 50% of infected nodes uniformly distributed over the contact network and 50% of + opinions uniformly distributed over the social network.

point is $\beta_{0.4}^c \simeq 0.58$ (see Fig. 3). Solid lines in Fig. 4 correspond to results for networks of size $N = 10^4$. As we can see, for $\beta > \beta_{0.4}^c \simeq 0.58$ the average value of $\rho_1(t)$ over many realizations, $\langle \rho_1(t) \rangle$, varies non-monotonically with time and asymptotically approaches a stationary value $\langle \rho_1^{\text{stat}} \rangle$ that depends on β , while $\langle \rho_1(t) \rangle$ decays to zero for $\beta < \beta_{0.4}^c$. That is, this non-monotonicity in $\langle \rho_1(t) \rangle$ makes $\langle \rho_1^{\text{stat}} \rangle$ jump from a value close to zero for $\beta < \beta_{0.4}^c$ ($\langle \rho_1^{\text{stat}} \rangle \simeq 0.0014$ for $\beta = 0.57$) to a much larger value for $\beta > \beta_{0.4}^c$ ($\langle \rho_1^{\text{stat}} \rangle \simeq 0.22$ for $\beta = 0.59$). We note that this peculiar non-monotonic temporal behavior is known to induce discontinuous transitions in social models with multiple states and constrains, like the Axelrod model (see for instance [31, 32]).

As we explain below, the origin of the non-monotonic behavior of $\langle \rho_1^{\text{stat}} \rangle$ is in the dynamic nature of the infection probability during each single realization, which can take two possible values: either the value $\beta p_d = 0$ a cross a contact link that overlaps with a $+-$ social link, or the value β otherwise (simulations correspond to $p_d = p_o = 0$). In other words, the infectivity across a given link $i - j$ may switch between 0 and β over time, depending on the opinion states of nodes i and j . This gives an average infection rate over the entire system that fluctuates according to the evolution of the fraction of $+-$ links, $\rho^{+-}(t)$, in one

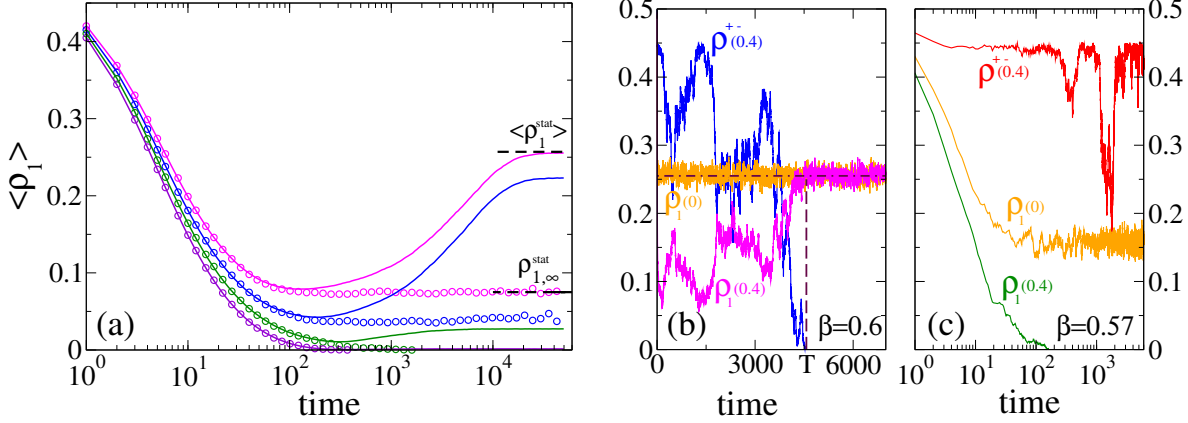


FIG. 4: (a) Time evolution of the average fraction of infected nodes $\langle \rho_1 \rangle$ on a bilayer system with coupling $q = 0.4$. Solid lines correspond to networks of size $N = 10^4$, while open circles are for networks with $N = 10^6$ nodes. Curves correspond to infection probabilities $\beta = 0.60, 0.59, 0.58$ and 0.57 (from top to bottom). Horizontal dashed lines indicate the stationary values for $\beta = 0.60$ and the two network sizes. (b) and (c) Evolution of the fraction of infected nodes, ρ_1 , and the fraction of $+-$ social links, ρ^{+-} , in two distinct realizations for $q = 0.4$ and $\beta = 0.6$ (b) and $\beta = 0.57$ (c). The evolution of ρ_1 is also shown for $q = 0$ in both panels.

realization. We shall exploit this observation in section IV to develop a mean-field approach for the evolution of the system. In panels (b) and (c) of Fig. 4 we plot ρ_1 and ρ^{+-} in a single realization of the dynamics, for $q = 0.4$ and two values of β . For $\beta = 0.60 > \beta_{0.4}^c$ [panel (b)] we observe that ρ_1 displays large variations up to a time $T \simeq 4570$ (vertical dashed line) where ρ^{+-} becomes 0, after which ρ_1 fluctuates around a stationary value $\rho_1^{\text{stat}} \simeq 0.255$ (horizontal dash-dotted line), while for $\beta = 0.57 < \beta_{0.4}^c$ [panel (c)] ρ_1 rapidly decays to zero, before ρ^{+-} reaches zero. When ρ^{+-} becomes zero [panel (b)] only $++$ or $--$ links remain and, therefore, the disease dynamics behaves as the one of the standard CP with infection probability $\beta = 0.6$ across all links, reaching the stationary value $\rho_1^{\text{stat}}(q = 0, \beta = 0.6) \simeq 0.255$. We can say that after time T the disease dynamics uncouples from the opinion dynamics. Indeed, panel (b) shows ρ_1 in a single realization on an isolated network ($q = 0$) with $\beta = 0.6$, where we observe a very quick decay to a stationary value that overlaps with the one for the coupled case $q = 0.4$. Therefore, as we can see in Fig. 3, the value of ρ_1^{stat} in the endemic phase of the coupled system ($\beta > \beta_{0.4}^c$) is the same as in the uncoupled case. Then, at the transition point $\beta_{0.4}^c \simeq 0.58 > \beta_0^c \simeq 0.53$, ρ_1^{stat} jumps from the

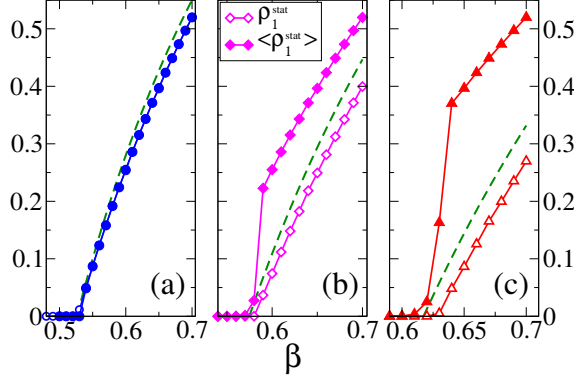


FIG. 5: Stationary density of infected nodes vs β , for couplings $q = 0$ (a), $q = 0.4$ (b) and $q = 0.7$ (c). Open symbols correspond to a single realization on a network of size $N = 10^6$, while filled symbols correspond to an average over 5000 realizations on networks of $N = 10^4$ nodes. In panel (a), open symbols overlap with filled symbols. Dashed curves represent the theoretical approximation from Eq. (11).

value $\rho_1^{\text{stat}}(q = 0, \beta_{0.4}^c) \simeq 0.22$ –corresponding to the uncoupled system– to the small value $\rho_1^{\text{stat}} \simeq 0.027$, showing a discontinuous change. This particular behavior of ρ_1^{stat} is the origin of the discontinuous transitions for $q > 0$ shown in Fig. 3.

The results described above correspond to networks of size $N = 10^4$, where finite-size fluctuations ultimately drive the system to an absorbing state in which all nodes are susceptible ($\rho_1 = 0$) and have either opinion $+$ or $-$ ($\rho^{+-} = 0$), i.e., an opinion consensus on a completely healthy population. Fluctuations play a fundamental role in the discontinuous nature of the transition because, as we discussed previously, the stationary value of ρ_1 in a single realization depends on whether ρ^{+-} becomes zero before ρ_1 does. However, this behavior does not hold in the thermodynamic limit, where finite-size fluctuations vanish and the transition turns into continuous, as we explain next. In order to investigate this phenomenon, we run simulations on very large networks. Open circles in Fig. 4 correspond to single realizations on a network of $N = 10^6$ nodes, for the same values of β as for networks with $N = 10^4$ nodes (solid lines). We observe that curves for $N = 10^6$ decay monotonically with time to a stationary value denoted by $\rho_{1,\infty}^{\text{stat}}$ (only shown for $\beta = 0.6$), which agrees with the minimum of the non-monotonic curves for $N = 10^4$. We need to note that these states are not truly stationary, in the sense that ρ_1 exhibits a very long plateau (outside the shown scale) but eventually increases and reaches the same stationary value $\langle \rho_1^{\text{stat}} \rangle$ of the curves

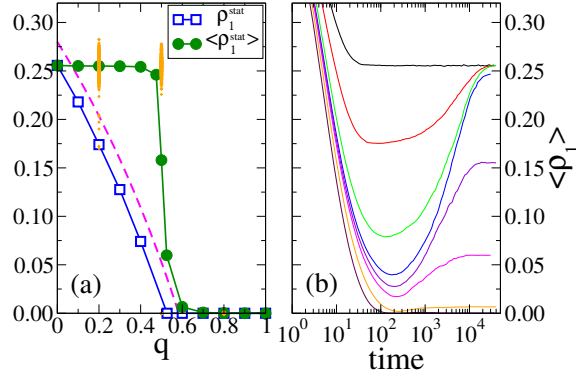


FIG. 6: (a) Stationary fraction of infected nodes ρ_1^{stat} vs coupling q , for $\beta = 0.6$. Solid circles correspond to the average of ρ_1^{stat} over 5000 realizations on networks with $N = 10^4$ nodes. Some of the values of ρ_1^{stat} in a single realization are shown by dots, for $q = 0.2, 0.5$ and 0.8 . Empty squares represent results of ρ_1^{stat} in a single realization on a network of size $N = 10^6$. The dashed curve is the theoretical approximation from Eq. (11). (b) Time evolution of $\langle \rho_1 \rangle$ for couplings $q = 0, 0.2, 0.4, 0.475, 0.5, 0.525, 0.6$ and 0.7 (from top to bottom) on networks of size $N = 10^4$.

for $N = 10^4$. We have checked that the time taken to reach this stationary state diverges with N , and thus is never reached in the $N \rightarrow \infty$ limit. Therefore, we take $\rho_{1,\infty}^{\text{stat}}$ as the stationary value in the thermodynamic limit. In Fig. 5 we compare $\rho_{1,\infty}^{\text{stat}}$ (open symbols) and ρ_1^{stat} (filled symbols) for three values of q , where we observe that ρ_1^{stat} decays continuously as β decreases and becomes zero at the same value β_q^c of the transition in finite systems. That is, the healthy-endemic transition is continuous in the thermodynamic limit. In section IV we develop a mean-field approach that allows to estimate the stationary fraction of infected nodes ρ_1 [see Eq. (11)]. The theoretical approximation from Eq. (11) –shown as a dashed curve in each panel of Fig. 5– agrees reasonable well with numerical results on the largest network of size $N = 10^6$ (filled symbols), even though the agreement worsens as q gets larger. As explained in section IV, the theory corresponds to the $N \rightarrow \infty$ limit, which confirms that the transition is continuous in infinite large systems.

Up to here we studied the response of the system when the infection probability is varied, for a fixed coupling. We now explore the effects of having a varying coupling on disease prevalence. In Fig. 6(a) we plot $\langle \rho_1^{\text{stat}} \rangle$ on two coupled networks of $N = 10^4$ nodes (circles), and ρ_1^{stat} in a single realization on networks of size $N = 10^6$ (squares), as a function of the

coupling q , for $\beta = 0.6$. The upper curve for $N = 10^4$ shows an abrupt transition from an endemic to a healthy phase as the coupling overcomes a threshold value $q_{0.6}^c \simeq 0.5$. To explore this behavior in more detail, we show with dots the value of ρ_1^{stat} in every single realization for three values of q . For $q = 0.2$, all dots fall around its mean value $\langle \rho_1^{\text{stat}} \rangle \simeq 0.26$, while for $q = 0.8$ they are at $\rho_1^{\text{stat}} = 0$. At the transition point $q_{0.6}^c$ the distribution of dots is bimodal, i.e., dots are around $\rho_1^{\text{stat}} \simeq 0.26$ and at $\rho_1^{\text{stat}} = 0$, giving an average value $\langle \rho_1^{\text{stat}} \rangle \simeq 0.165$. This distribution shows that the system is bistable around the transition point, a clear evidence of a discontinuous transition. The reason for this discontinuity is the non-monotonic time evolution of $\langle \rho_1 \rangle$ [see Fig. 6(b)], similarly to what happens when β is varied, as shown before. The only difference with this previous studied case is that, as β is fixed, the stationary value of ρ_1 in single realizations does not change with q , but is either $\rho_1^{\text{stat}} = 0$ or $\rho_1^{\text{stat}} \simeq 0.26$, in agreement with the binomial distribution. The former situation happens in realizations where ρ_1 hits zero before ρ^{+-} does, while the later corresponds to realizations where ρ^{+-} becomes zero and thus the two dynamics get uncoupled, after which ρ_1 reaches a stationary value similar to 0.26 corresponding to $q = 0$.

Figure 6(a) shows that the transition with q becomes continuous in the thermodynamic limit (squares), where the transition point is similar to the one for finite systems $q_{0.6}^c \simeq 0.5$. One can also check that the stationary value ρ_1^{stat} for a given q in the thermodynamic limit agrees with the minimum of the corresponding $\langle \rho_1 \rangle$ vs time curve of Fig. 6(b). This behavior is akin to the one shown in Fig. 4(a).

The $\beta - q$ phase diagram of Fig. 7 summarizes the results obtained in this section, on how the coupling between the contact and social networks affects the prevalence of the disease. By increasing the coupling q it is possible to bring an initially uncoupled system from the endemic to the healthy phase (vertical arrow). Also, as the coupling increases, a larger infection probability β is needed to pass from the healthy to the endemic phase (horizontal arrow).

Finally, we reproduced the phase diagram for various values of the probability p_d of having a successful infection across $+-$ links, and the probability p_o of opinion imitation between infected neighbors (inset of Fig. 7). We see that the orientation of the transition line that separates the healthy from the endemic phase becomes more vertical as p_d increases, enlarging the endemic phase, as we might expect. And when $p_d = 1.0$, the transition becomes independent on the coupling q and p_o (the curve is the same for all values of p_o). We also

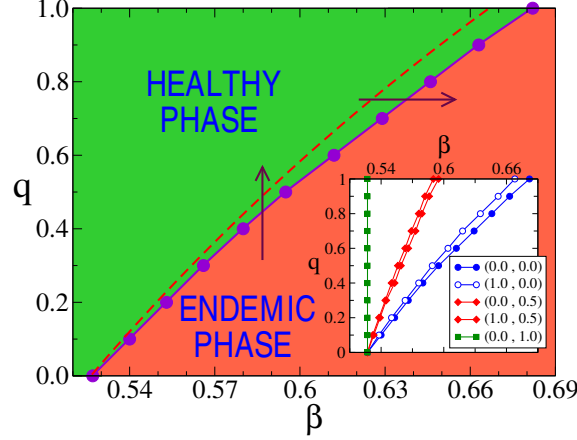


FIG. 7: Phase diagram of the contact process coupled to the voter model, showing the healthy and endemic phases in the $\beta - q$ space, with $p_o = p_d = 0$. The dashed curve represents the analytical approximation of the transition line from Eq. (13). The inset shows the transition lines for the set of values (p_o, p_d) indicated in the legend. For $p_d = 1.0$ (squares), the transition is given by the vertical line $\beta \simeq 0.53$ for all values of p_o (only $p_o = 0.0$ shown).

observe a slight decrease of the healthy phase when p_o increases while keeping β fixed. As the fraction of $+-$ links decreases faster when opinions are copied at a higher rate, one expects an increase of the effective infection rate and, consequently, an enlargement of the endemic phase.

B. Effects of disease spreading on opinion consensus

In this section we explore how the spreading of the disease affects the dynamics of opinions. As the transmission of opinions between neighboring nodes is more difficult when at least one of them is sick, we are particularly interested in studying up to what extent the disease slows down opinion diffusion over the social network, and how that depends on q , β , p_o and p_d . A way to quantify this is by looking at the time to reach opinion consensus. In Fig. 8 we show how the mean consensus time τ varies with the coupling q , for infection probability $\beta = 0.6$ and various values of p_o and p_d . For a better comparison with the voter model on an isolated network, τ is normalized by the mean consensus time τ_0 when the networks are uncoupled ($q = 0$). Symbols correspond to MC simulations, while solid lines are the analytical approximations from Eq. (17) obtained in section IV. Here we present

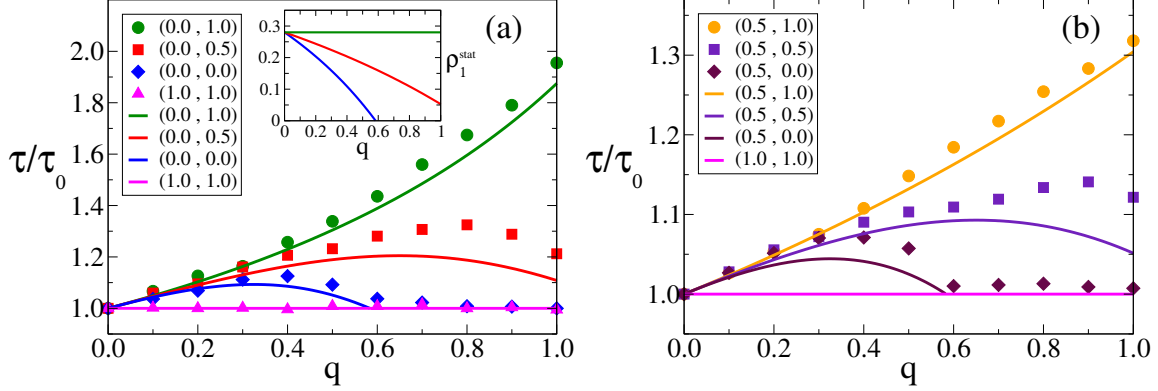


FIG. 8: (Color online) Mean time τ to reach opinion consensus on the social network as a function of the coupling q with the contact network, normalized by the mean consensus time in the absence of coupling τ_0 . The infection probability in the contact network is $\beta = 0.6$. Each network has $N = 10^4$ nodes and mean degree $\mu = 10$. The average was done over 5000 independent realizations. Different symbols correspond to numerical results for the set of values (p_o, p_d) indicated in the legends [(a) for $p_o = 0.0$ and (b) for $p_o = 0.5$], while solid lines are the corresponding analytical approximations from Eq. (17). For comparison, we also show in both panels numerical data and the analytical curve for the uncoupled case $(p_o, p_d) = (1.0, 1.0)$. Inset of panel (a): ρ_1^{stat} vs q from Eq. (10) for $p_d = 1.0, 0.5$ and 0.0 (from top to bottom).

results for β above the critical point of an isolated network $\beta_0^c \simeq 0.53$ because for $\beta < \beta_0^c$ the effects of disease on consensus times are negligible. This happens because for $\beta < \beta_0^c$ and any value of q the disease quickly disappears on the contact network and, as all nodes are susceptible, the dynamics of opinions is decoupled from the disease dynamics, reaching consensus in a time very similar to the one in the uncoupled case ($\tau \simeq \tau_0$).

We observe in Fig. 8 that the q -dependence of τ is quite diverse, showing monotonic as well as non-monotonic behaviors. This is as a consequence of the competition between two different mechanisms that directly affect opinion transmission. One is the link overlap between the two networks that is proportional to q , and the other is the disease prevalence that decreases with q , as we explain below. The opinion transmission through a social link that overlaps with a contact link is slowed down, in average, by a factor $1/p_o$ when at least one of the two nodes is infected. Therefore, the overall delay in opinion transmission caused by the total overlap tends to increase with q , and so does τ . This effect explains the initial

monotonic increase of τ as q increases from 0, in all curves. However, as q becomes larger a second effect becomes important: the fraction of infected nodes decreases with q [see inset of Fig. 8(a)], due to the coupling with the opinion dynamics that reduces the effective infection probability as discussed in section III A. Then, lower disease prevalence translates into fewer social links affected by the disease and, therefore, into a smaller opinion delay. This effect tends to reduce τ with q .

With these two mechanisms at play, the shapes of curves in Fig. 8 for different values of p_o and p_d can be qualitatively explained in terms of the combined effects of overlap and prevalence. For instance, in Fig. 8(a) we observe that the three curves for $p_o = 0.0$ have a quite different behavior. For $p_d = 1.0$ the effect of prevalence does not vary with q , given that ρ_1^{stat} is independent of q [inset of Fig. 8(a)]. Then, τ increases monotonically with q as the overlap increases. For $p_d = 0.5$ the prevalence effect increases with q (ρ_1^{stat} decreases), becoming dominant for q above 0.8 when τ decays, and leading to a non-monotonic behavior of τ vs q . Finally, for $p_o = 0.0$ we observe a non-monotonicity similar than that of the $p_d = 0.5$ curve, but with the addition that τ becomes very similar to τ_0 for all values of $q > 0.6$. This is because ρ_1^{stat} becomes zero above $q \simeq 0.583$ and thus the disease has no effect on opinions, leading to consensus times similar to the ones measured in isolated networks. These behaviors for the $p_o = 0.0$ case are also observed for other values of p_o , as we show in Fig. 8(b) for $p_o = 0.5$. We see that shape of the curves for $p_d = 0.0, 0.5$ and 1.0 are analogous to the ones of Fig. 8(a) for the corresponding values of p_d . However, consensus times are smaller for the $p_o = 0.5$ case because the delay in opinion transmission is reduced as p_o increases.

In Fig. 9 we plot the normalized mean consensus time τ/τ_0 as a function of the infection probability β obtained from Eq. (17). Panels (a) and (b) correspond to couplings $q = 0.5$ and $q = 1.0$, respectively. To analyze these plots we recall that, as explained above, consensus times increase with the level of disease prevalence in the contact network, given that a larger disease prevalence translates into a larger delay in opinion propagation and in the subsequent consensus. A first simple observation is that τ increases with β and also with p_d , as we expect from the fact that a larger value of β and p_d implies a larger disease prevalence. A second observation is that τ decreases with the likelihood of opinion transmission p_o , as explained before when we compared τ in Fig. 8(a) with Fig. 8(b). A third observation is that τ approaches a value independent on p_d when β goes to 1.0. This is because for $\beta = 1.0$

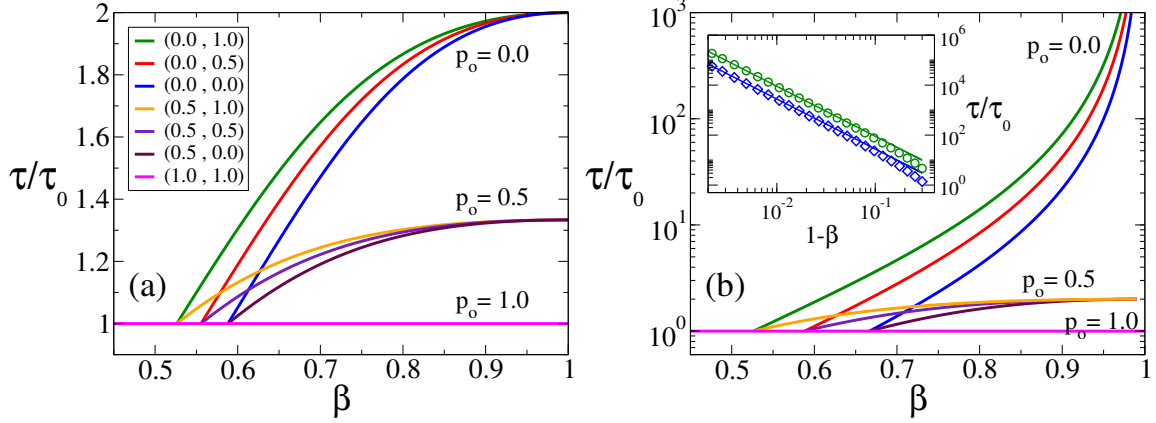


FIG. 9: (Color online) Normalized mean consensus time τ/τ_0 on the social network as a function of the infection probability β on the contact network for the same network parameters as in Fig. 8, coupling $q = 0.5$ (a) and $q = 1.0$ (b). Curves correspond to Eq. (17) for different values of the set (p_o, p_d) with the same color code as in Fig. 8, and indicated in the legend of panel (a). Curves for the sets (1.0, 0.0) and (1.0, 0.5) overlap with the curve for (1.0, 1.0) shown as the horizontal line $\tau/\tau_0 = 1$. The inset of panel (b) shows the divergence of τ as β approaches 1.0, when $q = 1.0$, $p_o = 0.0$, and $p_d = 1.0$ (circles) and $p_d = 0.0$ (diamonds). Solid lines are the approximations from Eq. (17).

(recovery probability equals zero) and a fixed value of q and p_o all nodes are infected at the stationary state, independently on the value of p_d , and thus consensus times are the same for all p_d . As we see in Fig. 9(b), the case $q = 1$ and $p_o = 0$ is special because τ diverges as β approaches 1.0. This happens because in this situation the transmission of opinions is only possible between connected nodes that are both susceptible, which vanish in the $\beta \rightarrow 1.0$ limit, leading to divergent consensus times. A rough estimation of how τ scales with β can be obtained by assuming that τ is proportional to the time scale associated to the opinion transmission across two given neighboring nodes in the social network, i and j , with opinions $+$ and $-$, respectively. As $q = 1$, i and j are also neighbors in the contact network. Starting from a situation where i and j are infected for high β , the opinion transmission happens after both nodes recover. Therefore, τ is determined by the time it takes the 1–1 contact link to become a 0–0 link, which scales as $(1 - \beta)^{-2}$. In section IV we derived a more accurate expression for τ that exhibits this quadratic divergence in the $\beta \rightarrow 1$ limit, shown in the inset of Fig. 9(b) by solid lines.

IV. ANALYTICAL APPROACH

In order to gain an insight into the behavior of the two-layer system described in section III, we develop here a mean-field (MF) approach that allows to study the time evolution of the system in terms of the global densities of nodes and links in different states. We denote by ρ^+ and ρ^- the fractions of nodes with $+$ and $-$ opinion in the social network, respectively, and by ρ_1 and ρ_0 the fractions of infected and susceptible nodes in the contact network, respectively. The fractions of social links between $+$ and $-$ opinion nodes are denoted by ρ^{+-} , while ρ_{10} represents the fraction of contact links between infected and susceptible nodes. An analogous notation is used for $++$ and $--$ social links and for 1-1 and 0-0 contact links. The fractions of nodes ρ^+ and ρ_1 are normalized with respect to the number of nodes N in each network, while the fractions of links ρ^{+-} and ρ_{10} are normalized by the number of links $\mu N/2$ in each network, with mean degree $\mu = \langle k \rangle$. Given that the number of nodes and links are conserved in each layer, the following conservation relations hold at any time for the social layer

$$1 = \rho^+ + \rho^-, \quad (1a)$$

$$1 = \rho^{++} + \rho^{--} + \rho^{+-}, \quad (1b)$$

$$\rho^+ = \rho^{++} + \frac{1}{2}\rho^{+-}, \quad (1c)$$

$$\rho^- = \rho^{--} + \frac{1}{2}\rho^{+-}, \quad (1d)$$

and analogously for the contact layer

$$1 = \rho_1 + \rho_0, \quad (2a)$$

$$1 = \rho_{11} + \rho_{00} + \rho_{10}, \quad (2b)$$

$$\rho_1 = \rho_{11} + \frac{1}{2}\rho_{10}, \quad (2c)$$

$$\rho_0 = \rho_{00} + \frac{1}{2}\rho_{10}. \quad (2d)$$

In appendices A, B, C and D we derive the following set of ordinary differential equations for ρ^+ , ρ^{+-} , ρ_1 and ρ_{10} , respectively:

$$\frac{d\rho^+}{dt} = 0, \quad (3a)$$

$$\frac{d\rho^{+-}}{dt} = \frac{2\omega\rho^{+-}}{\mu} \left[(\mu - 1) \left(1 - \frac{\rho^{+-}}{2\rho^+(1 - \rho^+)} \right) - 1 \right], \quad (3b)$$

with

$$\omega \equiv 1 - q(1 - p_o) \left(\rho_1 + \frac{\rho_{10}}{2} \right), \quad (4)$$

and

$$\frac{d\rho_1}{dt} = \frac{\gamma\beta\rho_{10}}{2} - (1 - \beta)\rho_1, \quad (5a)$$

$$\frac{d\rho_{10}}{dt} = \frac{\gamma\beta\rho_{10}}{\mu} \left[(\mu - 1) \left(1 - \frac{\rho_{10}}{1 - \rho_1} \right) - 1 \right] + 2(1 - \beta)(\rho_1 - \rho_{10}), \quad (5b)$$

with

$$\gamma \equiv 1 - q(1 - p_d)\rho^{+-}. \quad (6)$$

These equations represent an approximate mathematical description of the time evolution of the model on infinitely large networks, where finite-size fluctuations are neglected. For the sake of simplicity, we assumed in the derivation that all nodes have the same number of neighbors $k = \mu$ chosen at random, which is equivalent to assuming that networks are degree-regular random graphs. However, we expect this approximation to work well in networks with homogeneous degree distributions like the ER networks we used in the MC simulations. We also implemented an homogeneous pair approximation [30] that takes into account correlations between the state of neighboring nodes within the same layer (intralayer pair approximation), but neglects correlations between opinion and disease states of both layers (interlayer annealing approximation). That is, we considered that the opinion state of each node is uncorrelated with its own disease state and with its neighbors' disease states and, conversely, that its disease state is uncorrelated with its own and its neighbors' opinion states.

It is instructive to analyze the structure of Eqs. (3) and (5). Equations (3) describe the evolution of opinions on the social layer. From Eq. (3a) we see that the fraction of + nodes is conserved over time: $\rho^+(t) = \rho^+(t = 0)$ for all $t \geq 0$. This behavior is reminiscent of that of the VM on isolated topologies, where opinion densities are conserved at each time step. It seems that the disease dynamics is not able to break the intrinsic symmetry of opinion states induced by the voter dynamics. Equation (3b) for the evolution of ρ^{+-} has a extra prefactor ω compared to the corresponding equation for the VM on isolated networks [30], which reveals that the disease affects the dynamics of opinions through its prevalence level, expressed by ρ_1 and ρ_{10} [see Eq. (4)]. As discussed in appendix A, ω can be interpreted

as the “effective probability” that a node i adopts the opinion of a chosen social neighbor j with opposite opinion, which depends on the disease state of both i and j . Within a MF approach, we can assume that the probability that i copies j ’s opinion depends on the disease state of an “average pair” of contact neighbors, and that this probability is the same for all social neighbors. In these terms, ω becomes the average copying probability over the entire social network. Indeed, we can check that the average value of ω over the three possible connection and disease state configurations of a contact pair

$$\omega = \begin{cases} 1 & \text{with probability } 1 - q \text{ (no disease link),} \\ 1 & \text{with probability } q \rho_{00} \text{ (0-0 disease link),} \\ p_o & \text{with probability } q(1 - \rho_{00}) \text{ (either 10, 01 or 1-1 disease link),} \end{cases}$$

gives $\omega = 1 - q + q[\rho_{00} + (1 - \rho_{00})p_o]$, which is reduced to Eq. (4) by using the relation $1 - \rho_{00} = \rho_1 + \rho_{10}/2$ that follows from Eqs. (2b) and (2c). As we see, the overall effect of the disease on the opinion dynamics at the MF level is to reduce by a factor ω the rate at which opinions change in each node. This effect slows down the propagation of opinions through the social network, but it does not seem to alter the properties of the voter dynamics.

Equations (5) describe the evolution of the disease on the contact layer. These equations have the same form as the corresponding equations for the CP on an isolated network within the homogeneous pair approximation [7], but with a probability of infection given by $\gamma\beta \leq \beta$. In analogy to the case of ω described above, $\gamma\beta$ can be interpreted as the “effective probability” that a given infected node i transmits the disease to a susceptible neighbor j on the contact layer, which depends on the opinions of both i and j . Indeed, the expression $\gamma\beta = [1 - q(1 - p_d)\rho^{+-}]\beta$ from Eq. (6) is the average infection probability on the contact network, calculated over the three possible connection and opinion state configurations of a social pair:

$$\text{infection probability} = \begin{cases} \beta & \text{with prob. } 1 - q \text{ (no social link),} \\ \beta & \text{with prob. } q(1 - \rho^{+-}) \text{ (either ++ or -- social link),} \\ p_d \beta & \text{with prob. } q\rho^{+-} \text{ (+- social link).} \end{cases}$$

Thus, our MF approach assumes that this “effective infection probability” from i to j depends on the opinion states of an “average pair” of neighbors on the social layer, and that is the same for all contact neighbors. We can say that, at the MF level, the disease dynamics

follows the standard CP on a single isolated network with homogeneous infection probability $\gamma\beta$ and recovery probability $1 - \beta$ in each node. Therefore, the dynamics of opinions has an effect on the disease dynamics equivalent to that of an external homogeneous field acting on each node of the contact network, reducing the probability of infection between neighbors by a factor γ , while keeping the same recovery probability.

In the next two subsections we derive analytical expressions for the disease prevalence ρ_1^{stat} and the mean consensus time τ , from the system of Eqs. (3-6).

A. Disease prevalence

In order to study how the opinion dynamics affects the disease prevalence, we find the fraction of infected nodes at the stationary state ρ_1^{stat} from Eqs. (3) and (5). We start by setting the four time derivatives to zero, substituting ρ_{10} by $2(1 - \beta)\rho_1/\gamma\beta$ from Eq. (5a) into Eq. (5b), and solving for ρ_1 . After doing some algebra we obtain two solutions, but only one is stable depending on the values of the parameters. The non-trivial solution

$$\rho_1^{\text{stat}} = \frac{[(\mu - 1)\gamma + \mu]\beta - \mu}{[(\mu - 1)\gamma + 1]\beta - 1} \quad (7)$$

corresponds to the endemic phase, where a fraction of nodes is infected, and is stable only when the numerator $\lambda \equiv [(\mu - 1)\gamma + \mu]\beta - \mu$ is larger than zero. For $\lambda < 0$ the stable solution is $\rho_1^{\text{stat}} = 0$, corresponding to the healthy phase where all nodes are susceptible, while $\lambda = 0$ indicates the transition point between the endemic and the healthy phase. The expression for ρ_1^{stat} from Eq. (7) is still not closed because it depends on ρ^{+-} , through the prefactor γ . From Eq. (3b) we see that the fraction of $+-$ social links reaches a stationary value given by the expression

$$\rho_{\text{stat}}^{+-} = \frac{2(\mu - 2)}{(\mu - 1)}\rho^+(0)[1 - \rho^+(0)], \quad (8)$$

where we used $\rho^+ = \rho^+(0)$ given that ρ^+ remains constant over time, as mentioned before. For a symmetric initial condition on the social layer ($\rho^+(0) = 1/2$), as the one used in the simulations, we have $\rho_{\text{stat}}^{+-} = (\mu - 2)/2(\mu - 1)$. Replacing this last expression for ρ_{stat}^{+-} in Eq. (6) we obtain the following expression for γ :

$$\gamma = 1 - \frac{q(1 - p_d)(\mu - 2)}{2(\mu - 1)}. \quad (9)$$

Finally, plugging Eq. (9) into Eq. (7) we arrive to the following approximate expression for the stationary fraction of infected nodes in the endemic phase:

$$\rho_1^{\text{stat}} = \frac{[2(2\mu - 1) - q(1 - p_d)(\mu - 2)] \beta - 2\mu}{[2\mu - q(1 - p_d)(\mu - 2)] \beta - 2}. \quad (10)$$

For a network of mean degree $\mu = 10$ and $p_d = 0$, Eq. (10) is reduced to the simple expression

$$\rho_1^{\text{stat}} = \frac{(19 - 4q) \beta - 10}{(10 - 4q) \beta - 1}, \quad (11)$$

which is plotted in Figs. 5 and 6 (dashed curves). These theoretical curves are in reasonable agreement with simulation results on very large networks (empty symbols). Figure 5 shows that ρ_1^{stat} from Eq. (11) continuously decreases and vanishes as β decreases beyond a threshold value, as it happens in the standard CP. This shows that the transition to the healthy state is continuous within the MF approach, which assumes that the system is infinite large. In Fig. 6 we see that ρ_1^{stat} decreases with q , reducing the prevalence and inducing a transition to the healthy phase. That is, Eq. (10) predicts a healthy-endemic continuous transition as β and q are varied, which happens at the point where ρ_1^{stat} vanishes, leading to the relation

$$[2(2\mu - 1) - q(1 - p_d)(\mu - 2)] \beta - 2\mu = 0. \quad (12)$$

The transition line

$$q_c = \frac{19\beta_c - 10}{4(1 - p_d)\beta_c} \quad (13)$$

obtained from Eq. (12) for $\mu = 10$ is plotted in Fig. 7 for $p_d = 0$ (dashed curve). We can see that the agreement with simulations is good for small values of the coupling q , but discrepancies arise as q increases, where the theoretical prediction from Eq. (13) overestimates numerical values. Another simple observation that follows from Eq. (13) is that for $\beta > 10/[19 - 4(1 - p_d)]$ we obtain the nonphysical value $q_c > 1$. This means that, in the network model, it is possible to induce a transition by increasing the coupling only when β is lower than a given value, as we see in Fig. 7 for $\beta < 0.68$.

As a final remark we stress that the transitions within this MF approach are continuous, in agreement with simulations in very large networks. This is so because Eqs. (3) and (5) correspond to an infinite large system where finite-size fluctuations are neglected.

B. Opinion consensus times

In this section we study the quantitative effects of the disease on the time to reach opinion consensus. For that, we find an analytical estimation of the mean consensus time τ as a function of the model parameters.

As mentioned in section IV, in infinitely large systems ρ^+ remains constant over time [see Eq. (3a)]. However, in finite systems ρ^+ fluctuates until it reaches either value $\rho^+ = 1$ (+ consensus) or $\rho^+ = 0$ (− consensus), with both configurations characterized by the absence of $+-$ social links ($\rho^{+-} = 0$). A typical evolution of ρ^{+-} towards the absorbing state can be seen in Fig. 4 (b) for $q = 0.4$ on networks with $N = 10^4$ nodes. That is, consensus is eventually achieved in finite systems due to the stochastic nature of the opinion dynamics, which leads the social network to a state where all nodes share the same opinion. In a single opinion update ρ^+ may increase or decrease by $1/N$ with the same probability $\omega\rho^{+-}/2$, calculated as the probability $\rho^{+-}/2$ that a node and an opposite-opinion neighbor are selected at random, times the probability ω of opinion adoption. Therefore, the stochastic dynamics of the VM can be studied by mapping ρ^+ into the position of a symmetric one-dimensional random walker on the interval $[0, 1]$, with a jumping probability proportional to $\omega\rho_{\text{stat}}^{+-}/2$ and a step length of $1/N$. Starting from a symmetric configuration with $N/2$ nodes with $+$ opinion ($\rho^+(0) = 1/2$), the walker reaches either absorbing point $\rho^+ = 1$ or $\rho^+ = 0$ in an average number of steps that scales as N^2 . Then, given that the walker makes a single step in an average number of attempts that scales as $1/\omega\rho_{\text{stat}}^{+-}$, and that the time increases by $1/N$ in each attempt, we find that the mean consensus time scales as

$$\tau \sim \frac{N}{\omega\rho_{\text{stat}}^{+-}}. \quad (14)$$

As we see in Eq. (8), ρ_{stat}^{+-} is independent on the disease dynamics. In particular, we notice that ω in Eq. (3b) does not change the stationary value of ρ^{+-} , which remains the same as in the original VM [30]. Therefore, the effects of the disease on τ enters only through the effective copying probability ω , which sets the time scale associated to opinion updates. From Eq. (4) we see that ω equals 1.0 when the layers are uncoupled ($q = 0$) or when $p_o = 1.0$, and thus the dynamics of opinions is exactly the same as that of the original VM. However, ω is smaller than 1.0 in the presence of coupling ($q > 0$) and $p_o < 1.0$, and thus the evolution of the dynamics is “slowed down” –in average– by a factor $1/\omega > 1.0$, given that opinions are copied at a rate that is ω times smaller than in the uncoupled case.

As a consequence, τ increases by a factor $1/\omega$ respect to the mean consensus time in the uncoupled case $\tau_0 = \tau(q = 0) \sim N/\rho_{\text{stat}}^{+-}$, that is

$$\frac{\tau}{\tau_0} \simeq \frac{1}{\omega}. \quad (15)$$

To obtain a complete expression for the ratio τ/τ_0 as a function of the model's parameters we express ω in terms of ρ_1^{stat} , by substituting into Eq. (4) the stationary value of ρ_{10} that follows from Eq. (5a), $\rho_{10}^{\text{stat}} = 2(1 - \beta)\rho_1^{\text{stat}}/\gamma\beta$. This leads to

$$\omega = 1 - q(1 - p_o) \left(1 + \frac{1 - \beta}{\gamma\beta} \right) \rho_1^{\text{stat}}. \quad (16)$$

In the healthy phase is $\rho_1^{\text{stat}} = 0$, thus $\omega = 1.0$ and $\tau = \tau_0$. In this case, the theory predicts that the disease has no effect on the time to consensus because there are no infected nodes that can affect the opinion dynamics. However, having a value $\rho_1^{\text{stat}} > 0$ of infected nodes in the endemic phase has the effect of reducing ω or, equivalently, increasing τ respect to τ_0 . Plugging into Eq. (16) the expressions for γ and ρ_1^{stat} from Eqs. (9) and (10), respectively, and reordering some terms, we obtain the following expression that relates τ and τ_0 in the endemic phase:

$$\frac{\tau}{\tau_0} \simeq \left[1 - \frac{q(1 - p_o) \{ 2(\mu - 1) - q(1 - p_d)(\mu - 2)\beta \} \{ [2(2\mu - 1) - q(1 - p_d)(\mu - 2)]\beta - 2\mu \}}{\beta \{ 2(\mu - 1) - q(1 - p_d)(\mu - 2) \} \{ [2\mu - q(1 - p_d)(\mu - 2)]\beta - 2 \}} \right]^{-1} \quad (17)$$

In Fig. 8 we plot in solid lines the ratio τ/τ_0 vs q from Eq. (17) for $\mu = 10$. Even though discrepancies with numerical results (symbols) increase with the coupling q , the analytic expression (17) is able to capture the different qualitative behavior of the consensus time for several combinations of p_o and p_d , as we describe below. For low values of p_d , there is a transition to the healthy phase when q overcomes a value $q_c < 1$ given by Eq. (13) and, therefore, $\tau = \tau_0$ for all $q > q_c$ [see $p_d = 0$ curves in the main plot and the inset of Fig. 8(a)]. As a consequence, τ/τ_0 exhibits a non-monotonic behavior with q , as we described in section IIIB. For higher values of p_d , the transition to the healthy phase does not happen for the physical values $q \leq 1$ used in the model's simulations, given that $q_c > 1$ from Eq. (13). In this case, τ may either increase monotonically with q for large p_d values (see $p_d = 1.0$ curves), or have a maximum at some intermediate value for medium p_d values (see $p_d = 0.5$ curves). As explained in section IIIB, the non-monotonicity is a consequence of the competition between the level of link overlap among the two layers –which increases with q – and the

disease prevalence –which decreases with q –. This competition can be seen quantitatively in Eq. (16) for ω , which has three factors that depend on q and affect τ . Besides the factor proportional to q , the factor $1/\gamma$ also increases with q , as seen from Eq. (9). But these two factors are balanced by ρ_1^{stat} , which decreases with q .

An interesting case is the one for full coupling $q = 1.0$ and $p_o = 0$, because τ from Eq. (17) diverges as β approaches 1.0. This happens in the model because when $\beta = 1.0$ once a node becomes infected it remains infected forever. Then, once all nodes become infected the opinion dynamics stops, as infected neighboring nodes cannot interchange opinions, and thus the social layer freezes in a mixed state of $+$ and $-$ opinions and consensus is never achieved. By doing a Taylor series expansion of expression (17) up to second order in the small parameter $\epsilon = 1 - \beta \ll 1$ we obtain, after some algebra,

$$\frac{\tau}{\tau_0} \simeq \frac{[9 - 4(1 - p_d)]^2}{90(1 - \beta)^2}, \quad (18)$$

where we used $\mu = 10$. Equation (18) shows that τ diverges as $(1 - \beta)^{-2}$ in the $\beta \rightarrow 1.0$ limit, as shown in the inset of Fig. 9(b). For $\beta = 1.0$ and $p_o = 0$, we can check from Eq. (17) that $\tau/\tau_0 \simeq 1/(1 - q)$, which shows the divergence of τ as the system approaches the fully coupled state $q = 1.0$.

V. SUMMARY AND CONCLUSIONS

We proposed a bilayer network system to explore the interplay between the dynamics of opinion formation and disease spreading in a population of individuals. We used the voter model and the contact process to simulate the opinion and the disease dynamics running on a social and contact network, respectively. These two networks share the same nodes and they are coupled by a fraction q of links in common. We found that, when the networks are coupled, one dynamics can dramatically change the properties of the other dynamics, as compared to the case of isolated networks.

The VM dynamics is able to change the order of the healthy-endemic phase transition observed in the CP as the infection probability increases, from a continuous transition for the uncoupled case to a discontinuous transition when the coupling q is larger than zero. The discontinuity jump, which increases with q , is associated to the non-monotonic time evolution of the fraction of infected nodes. This non-monotonicity is as a consequence of

the time-varying nature of the effective infection probability, which fluctuates over time according to the stochastic evolution of the fraction of $+-$ social links. The system also exhibits a discontinuous transition from an endemic to a healthy phase when the coupling overcomes a value q_c . The discontinuity can also be explained in terms of the non-monotonic evolution of the disease prevalence. However, these observations appear to be the result of finite-size effects, given that the transitions become continuous in infinite large networks. A mean-field approach confirms this phenomenon and shows that the disease dynamics is equivalent to that of the standard CP with an effective infection probability that is constant over time, and that decreases with the coupling and the stationary fraction of $+-$ social links.

On its part, the CP dynamics has the overall effect of slowing down the propagation of opinions, delaying the process of opinion consensus respect to the one observed in an isolated network. The MF approach reveals that the opinion dynamics corresponds to that of the standard VM model with a probability of opinion transmission that decreases with q and the disease prevalence. Depending on the parameters values, the mean consensus time τ can show a monotonic increase with q , as well as a non-monotonic behavior. An insight on these results was given by the MF approach, which allowed to obtain an approximate mathematical expression that relates τ with the parameters. This approach shows that the behavior of τ with q is the result of two different mechanisms at play: the overlap of social and contact links that tends to increase τ with q , which is counterbalanced by the fraction of infected nodes that tends to decrease τ with q .

The results presented in this article correspond to a particular initial state that consists on even fractions of $+$ and $-$ opinion states and even fractions of infected and susceptible states, uniformly distributed over the networks. As a future work, it might be worth studying different initial conditions that consider, for instance, uneven fractions of opinion and disease states that are initially correlated. Finally, it would be interesting to develop an analytical approach that accounts for correlations between opinion and disease states in different layers, which might help to understand the discrepancies we found with numerical results for high couplings.

ACKNOWLEDGMENTS

We thank Gabriel Baglietto and Didier Vega-Oliveros for helpful comments on the manuscript. We acknowledge financial support from CONICET (PIP 0443/2014).

Appendix A: Derivation of the rate equation for ρ^+

We denote by $[\mathcal{O}]_{\mathcal{D}}$ the state of a given node, where $\mathcal{O} = +, -$ and $\mathcal{D} = 1, 0$ are its opinion and disease states, respectively. Thus, there are four possible node states: $[\overset{+}{0}]$, $[\overset{+}{1}]$, $[\overset{-}{0}]$ and $[\overset{-}{1}]$. In a single time step of the dynamics, the transitions from state $[\overset{-}{\mathcal{D}}]$ to state $[\overset{+}{\mathcal{D}}]$ when a node switches opinion from $-$ to $+$ lead to a gain of $1/N$ in ρ^+ , while the transitions $[\overset{+}{\mathcal{D}}] \rightarrow [\overset{-}{\mathcal{D}}]$ when there is a $+$ to $-$ opinion change lead to a loss of $1/N$ in ρ^+ . Considering these four possible transitions, the average change of ρ^+ in a single time step of time interval $\Delta t = 1/N$ is described by the rate equation

$$\begin{aligned} \frac{d\rho^+}{dt} &= \left. \frac{d\rho^+}{dt} \right|_{-\rightarrow+} + \left. \frac{d\rho^+}{dt} \right|_{+\rightarrow-} \\ &= \frac{1}{1/N} \left[\Delta\rho^+ \Big|_{\overset{-}{0} \rightarrow \overset{+}{0}} + \Delta\rho^+ \Big|_{\overset{-}{1} \rightarrow \overset{+}{1}} + \Delta\rho^+ \Big|_{\overset{+}{0} \rightarrow \overset{-}{0}} + \Delta\rho^+ \Big|_{\overset{+}{1} \rightarrow \overset{-}{1}} \right], \end{aligned} \quad (\text{A1})$$

where for instance the term $\Delta\rho^+ \Big|_{\overset{-}{0} \rightarrow \overset{+}{0}}$ represents the average change of ρ^+ in a time step due to $[\overset{-}{0}] \rightarrow [\overset{+}{0}]$ transitions. In turn, $\Delta\rho^+ \Big|_{\overset{-}{0} \rightarrow \overset{+}{0}}$ has four contributions corresponding to the different social interactions that lead to the $[\overset{-}{0}] \rightarrow [\overset{+}{0}]$ transition. Thus, we can write

$$\Delta\rho^+ \Big|_{\overset{-}{0} \rightarrow \overset{+}{0}} = \Delta\rho^+ \Big|_{\overline{\overset{-}{00}} \rightarrow \overline{\overset{+}{00}}} + \Delta\rho^+ \Big|_{\overline{\overset{-}{00}} \rightarrow \overline{\overset{+}{00}}} + \Delta\rho^+ \Big|_{\overline{\overset{-}{01}} \rightarrow \overline{\overset{+}{01}}} + \Delta\rho^+ \Big|_{\overline{\overset{-}{01}} \rightarrow \overline{\overset{+}{01}}}, \quad (\text{A2})$$

and similarly for the $[\overset{-}{1}] \rightarrow [\overset{+}{1}]$ transition corresponding to the second term in Eq. (A1)

$$\Delta\rho^+ \Big|_{\overset{-}{1} \rightarrow \overset{+}{1}} = \Delta\rho^+ \Big|_{\overline{\overset{-}{10}} \rightarrow \overline{\overset{+}{10}}} + \Delta\rho^+ \Big|_{\overline{\overset{-}{10}} \rightarrow \overline{\overset{+}{10}}} + \Delta\rho^+ \Big|_{\overline{\overset{-}{11}} \rightarrow \overline{\overset{+}{11}}} + \Delta\rho^+ \Big|_{\overline{\overset{-}{11}} \rightarrow \overline{\overset{+}{11}}}. \quad (\text{A3})$$

Third and fourth terms in Eq. (A1) are obtained by interchanging symbols $+$ and $-$ in Eqs. (A2) and (A3), respectively, due to the symmetry between $+$ and $-$ opinion states. We notice that disease states remain the same after the interactions, as only a change in the social layer can lead to a change in ρ^+ . The first term in Eq. (A2) represents the average change in ρ^+ due to interactions in which a node i in state $[\overset{-}{0}]$ copies the opinion of one its social neighbors j in state $[\overset{+}{0}]$, changing the state of i to $[\overset{+}{0}]$. This interaction is schematically represented by the symbol $[\overline{\overset{-}{00}}]$, where the horizontal line over the opinion

symbols describes a social link between i and j . In the same way, the symbol $\begin{bmatrix} \overline{+} \\ \overline{0} \end{bmatrix}$ represents an interaction between a $\begin{bmatrix} - \\ 0 \end{bmatrix}$ node and a neighboring $\begin{bmatrix} + \\ 0 \end{bmatrix}$ node connected by both a social and a contact link that are indicated by horizontal lines on top of the respective symbols. The second, third and fourth terms in Eq. (A2) describe, respectively, the transitions due to an interaction of node i with a $\begin{bmatrix} + \\ 0 \end{bmatrix}$ social/contact neighbor, a $\begin{bmatrix} + \\ 1 \end{bmatrix}$ social neighbor and a $\begin{bmatrix} + \\ 1 \end{bmatrix}$ social/contact neighbor.

We now illustrate how to build an approximate expression for each term of Eq. (A2) for $\Delta\rho^+|_{\begin{bmatrix} - \\ 0 \end{bmatrix} \rightarrow \begin{bmatrix} + \\ 0 \end{bmatrix}}$. For the sake of simplicity, we assume that all nodes have the same number of neighbors $k = \mu$ chosen at random, which is equivalent to assuming that networks are degree-regular random graphs. However, we expect this approximation to work well in networks with homogeneous degree distributions like ER networks. The first term in Eq. (A2) can be written as

$$\Delta\rho^+|_{\begin{bmatrix} - \\ 0 \end{bmatrix} \rightarrow \begin{bmatrix} + \\ 0 \end{bmatrix}} = P\left(\begin{bmatrix} - \\ 0 \end{bmatrix}\right) \sum_{\{\mathcal{N}_0^-\}}^{\mu} M(\{\mathcal{N}_0^-\}, \mu) \frac{\mathcal{N}[\begin{bmatrix} \overline{+} \\ \overline{0} \end{bmatrix}]}{\mu} \frac{1}{N}, \quad (\text{A4})$$

which can be understood as the product of the different probabilities associated to each of the consecutive events that lead to the $\begin{bmatrix} - \\ 0 \end{bmatrix} \rightarrow \begin{bmatrix} + \\ 0 \end{bmatrix}$ transition in a time step, as we describe below. A node i with state $\begin{bmatrix} - \\ 0 \end{bmatrix}$ is chosen at random with probability $P\left(\begin{bmatrix} - \\ 0 \end{bmatrix}\right)$. If node i has $\mathcal{N}[\begin{bmatrix} \overline{+} \\ \overline{0} \end{bmatrix}]$ social neighbors in state $\begin{bmatrix} + \\ 0 \end{bmatrix}$, then one of these social neighbors j is randomly chosen with probability $\mathcal{N}[\begin{bmatrix} \overline{+} \\ \overline{0} \end{bmatrix}]/\mu$, after which i copies j ' opinion with probability 1.0 because there is no contact link between i and j . Finally, ρ^+ increases by $1/N$ when i switches opinion.

In order to consider all possible scenarios of having $\mathcal{N}[\begin{bmatrix} \overline{+} \\ \overline{0} \end{bmatrix}] = 0, 1, \dots, \mu$ social neighbors we sum over all possible neighborhood configurations represented by $\{\mathcal{N}_0^-\} \equiv \{\mathcal{N}[\begin{bmatrix} \overline{+} \\ \overline{0} \end{bmatrix}], \mathcal{N}[\begin{bmatrix} \overline{+} \\ \overline{0} \end{bmatrix}], \mathcal{N}[\begin{bmatrix} \overline{+} \\ \overline{0} \end{bmatrix}], \mathcal{N}[\begin{bmatrix} \overline{+} \\ \overline{0} \end{bmatrix}], \mathcal{N}[\begin{bmatrix} \overline{+} \\ \overline{1} \end{bmatrix}], \mathcal{N}[\begin{bmatrix} \overline{+} \\ \overline{1} \end{bmatrix}], \mathcal{N}[\begin{bmatrix} \overline{+} \\ \overline{1} \end{bmatrix}], \mathcal{N}[\begin{bmatrix} \overline{+} \\ \overline{1} \end{bmatrix}]\}$, weighted by the probability of each configuration $M(\{\mathcal{N}_0^-\}, \mu)$. Here we denote by $\mathcal{N}[\begin{bmatrix} \overline{0} \\ \overline{d} \end{bmatrix}]$ the number of $\begin{bmatrix} 0 \\ d \end{bmatrix}$ social neighbors and by $\mathcal{N}[\begin{bmatrix} \overline{+} \\ \overline{d} \end{bmatrix}]$ the number of $\begin{bmatrix} + \\ d \end{bmatrix}$ social/contact neighbors [see Fig. (10)]. The number of each type of neighbor is between 0 and μ , and thus the sum in Eq. (A4) include eight summations

$$\sum_{\{\mathcal{N}_0^-\}}^{\mu} \equiv \sum_{\substack{\mathcal{O}=+,- \\ \mathcal{D}=0,1}} \left(\sum_{\mathcal{N}[\begin{bmatrix} \overline{0} \\ \overline{d} \end{bmatrix}]=0}^{\mu} + \sum_{\mathcal{N}[\begin{bmatrix} \overline{+} \\ \overline{d} \end{bmatrix}]=0}^{\mu} \right)$$

over all combinations subject to the constraint

$$\sum_{\substack{\mathcal{O}=+,- \\ \mathcal{D}=0,1}} (\mathcal{N}[\begin{bmatrix} \overline{0} \\ \overline{d} \end{bmatrix}] + \mathcal{N}[\begin{bmatrix} \overline{+} \\ \overline{d} \end{bmatrix}]) = \mu.$$

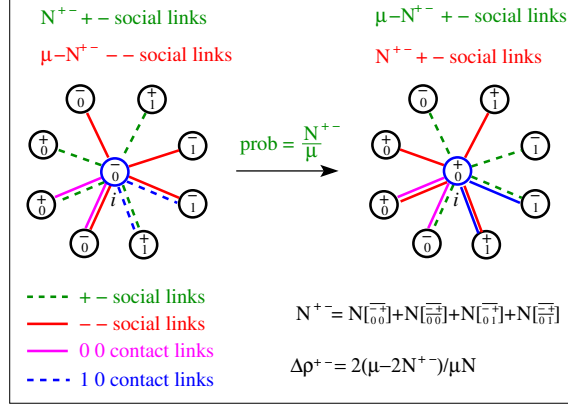


FIG. 10: (Color online) Schematic illustration of an opinion update in which a node i in state $\begin{bmatrix} - \\ 0 \end{bmatrix}$ changes to state $\begin{bmatrix} + \\ 0 \end{bmatrix}$ by copying the opinion $+$ of a randomly chosen neighbor (green dashed links). The change in the density of $+-$ links is denoted by $\Delta \rho^{+-}$.

In order to carry out the summation in Eq. (A4) we only take into account correlations between first neighbors, and neglect second and higher neighbor correlations (pair approximation). Thus, we define the probability $P[\begin{smallmatrix} \mathcal{O} \\ 0 \mathcal{D} \end{smallmatrix}] \equiv P(-\frac{\mathcal{O}}{\mathcal{D}} | \begin{smallmatrix} - \\ 0 \end{smallmatrix})$ that a given neighbor of node i is a social neighbor with state $\begin{bmatrix} \mathcal{O} \\ \mathcal{D} \end{bmatrix}$, and consider $P[\begin{smallmatrix} \mathcal{O} \\ 0 \mathcal{D} \end{smallmatrix}]$ to be conditioned to the state $\begin{bmatrix} - \\ 0 \end{bmatrix}$ of i only, and not on the other neighbors of i . Similarly, we denote by $P[\begin{smallmatrix} \mathcal{O} \\ 0 \mathcal{D} \end{smallmatrix}] = P(\frac{\mathcal{O}}{\mathcal{D}} | \begin{smallmatrix} - \\ 0 \end{smallmatrix})$ the conditional probability that a node connected to i is a social/contact neighbor with state $\begin{bmatrix} \mathcal{O} \\ \mathcal{D} \end{bmatrix}$, given that i has state $\begin{bmatrix} - \\ 0 \end{bmatrix}$. Therefore, M becomes the multinomial probability distribution defined as

$$M(\{\mathcal{N}_0^-\}, \mu) \equiv \begin{cases} \frac{\mu!}{\prod_{\mathcal{D}=0,1} \mathcal{N}[\begin{smallmatrix} \mathcal{O} \\ \mathcal{D} \end{smallmatrix}]! \mathcal{N}[\begin{smallmatrix} \mathcal{O} \\ \mathcal{D} \end{smallmatrix}]!} \prod_{\mathcal{D}=0,1} P[\begin{smallmatrix} \mathcal{O} \\ \mathcal{D} \end{smallmatrix}]^{\mathcal{N}[\begin{smallmatrix} \mathcal{O} \\ \mathcal{D} \end{smallmatrix}]} P[\begin{smallmatrix} \mathcal{O} \\ \mathcal{D} \end{smallmatrix}]^{\mathcal{N}[\begin{smallmatrix} \mathcal{O} \\ \mathcal{D} \end{smallmatrix}]} & \text{when } \sum_{\mathcal{D}=0,1} (\mathcal{N}[\begin{smallmatrix} \mathcal{O} \\ \mathcal{D} \end{smallmatrix}] + \mathcal{N}[\begin{smallmatrix} \mathcal{O} \\ \mathcal{D} \end{smallmatrix}]) = \mu; \\ 0 & \text{otherwise,} \end{cases}$$

where we have used the symbols $[\begin{smallmatrix} \mathcal{O} \\ \mathcal{D} \end{smallmatrix}]$ and $[\begin{smallmatrix} \mathcal{O} \\ \mathcal{D} \end{smallmatrix}]$ as short notations for $[\begin{smallmatrix} - & \mathcal{O} \\ 0 & \mathcal{D} \end{smallmatrix}]$ and $[\begin{smallmatrix} - & \mathcal{O} \\ 0 & \mathcal{D} \end{smallmatrix}]$, respectively. Then, performing the summation in Eq. (A4) we arrive to

$$\Delta \rho^+ \Big|_{\begin{smallmatrix} - & + \\ 0 & 0 \end{smallmatrix} \rightarrow \begin{smallmatrix} - & + \\ 0 & 0 \end{smallmatrix}} = \frac{P(\begin{smallmatrix} - \\ 0 \end{smallmatrix}) \langle \mathcal{N}[\begin{smallmatrix} - & + \\ 0 & 0 \end{smallmatrix}] \rangle}{\mu N} = \frac{P(\begin{smallmatrix} - \\ 0 \end{smallmatrix}) P[\begin{smallmatrix} - & + \\ 0 & 0 \end{smallmatrix}]}{N}, \quad (\text{A5})$$

where we have used the identity $\langle \mathcal{N}[\begin{smallmatrix} - & + \\ 0 & 0 \end{smallmatrix}] \rangle = \mu P[\begin{smallmatrix} - & + \\ 0 & 0 \end{smallmatrix}]$ for the mean value of $\mathcal{N}[\begin{smallmatrix} - & + \\ 0 & 0 \end{smallmatrix}]$. The other three terms in Eq. (A2) can be obtained following an approach similar to the one above for

$\Delta\rho^+ \Big|_{\substack{-+ \\ 0\ 0} \rightarrow \substack{++ \\ 0\ 0}}$, leading to the expression

$$\Delta\rho^+ \Big|_{\substack{-+ \\ 0\ 0} \rightarrow \substack{++ \\ 0\ 0}} = \frac{P(\substack{- \\ 0})}{N} (P[\substack{++ \\ 0\ 0}] + P[\substack{+- \\ 0\ 0}] + P[\substack{-+ \\ 0\ 1}] + p_o P[\substack{++ \\ 0\ 1}]), \quad (\text{A6})$$

where the prefactor p_o in the last term accounts for the probability of copying the opinion of an infected contact neighbor. Keeping in mind that we aim to obtain a closed system of rate equations for ρ^+ , ρ_1 , ρ^{+-} and ρ_{10} , we now find approximate expressions for the different probabilities of Eq. (A6) in terms of the fractions of nodes and links in each layer. We start by assuming that correlations between opinion and disease states of a given node are negligible, and thus we can write

$$P(\substack{- \\ 0}) \simeq \rho^- \rho_0. \quad (\text{A7})$$

Then, to estimate the conditional probabilities $P[\substack{++ \\ 0\ \mathcal{D}}]$ and $P[\substack{+- \\ 0\ \mathcal{D}}]$ it proves convenient to split each of them into two conditional probabilities

$$\begin{aligned} P[\substack{++ \\ 0\ \mathcal{D}}] &= P(\substack{-\ + \\ \mathcal{D}\ | \ 0}) = P(\substack{- \\ \mathcal{D}} | \substack{- \\ 0}) P(\substack{+ \\ \mathcal{D}} | \substack{- \\ 0}), \\ P[\substack{+- \\ 0\ \mathcal{D}}] &= P(\substack{-\ + \\ \mathcal{D}\ | \ 0}) = P(\substack{- \\ \mathcal{D}} | \substack{- \\ 0}) P(\substack{+ \\ \mathcal{D}} | \substack{- \\ 0}), \end{aligned}$$

using the relation $P(a, b|c) = P(a|c)P(b|a, c)$ and interpreting the entire event of connecting a given type of link to a $\substack{+ \\ \mathcal{D}}$ node as two separate events. Assuming that the type of link connected to node i is uncorrelated with the state of i , we have

$$\begin{aligned} P(\substack{- \\ \mathcal{D}} | \substack{- \\ 0}) &\simeq P(\substack{- \\ \mathcal{D}}) = 1 - q \quad \text{and} \\ P(\substack{- \\ \mathcal{D}} | \substack{- \\ 0}) &\simeq P(\substack{- \\ \mathcal{D}}) = q, \end{aligned}$$

and that opinion and disease states are uncorrelated as mentioned above, we have

$$\begin{aligned} P(\substack{+ \\ \mathcal{D}} | \substack{- \\ 0}) &\simeq P(+|--) P(\mathcal{D} | -) \quad \text{and} \\ P(\substack{+ \\ \mathcal{D}} | \substack{- \\ 0}) &\simeq P(+|--) P(\mathcal{D} | -). \end{aligned}$$

Within an homogeneous pair approximation [30], the probability $P(+|--)$ that a social neighbor j of a node i with opinion $\mathcal{O}_i = -$ has opinion $\mathcal{O}_j = +$ can be estimated as the ratio between the total number $\mu N \rho^{+-}/2$ of links from $-$ to $+$ nodes and the total number $\mu N \rho^-$ of links connected to $-$ nodes, that is $P(+|--) \simeq \rho^{+-}/2\rho^-$. Similarly, we estimate the probability that a contact neighbor j of a susceptible node has disease state $\mathcal{D}_j = 0$ as

$P(0|0) \simeq \rho_{00}/\rho_0$, and disease state $\mathcal{D}_j = 1$ as $P(1|0) \simeq \rho_{10}/2\rho_0$. And if j is not a neighbor of i on the contact layer then $P(\mathcal{D}|0) \simeq \rho_{\mathcal{D}}$. Assembling all these factors we obtain

$$\begin{aligned} P[\overline{+}] &\simeq \frac{(1-q)\rho^{+-}\rho_0}{2\rho^-}, & P[\overline{+}] &\simeq \frac{q\rho^{+-}\rho_{00}}{2\rho^-\rho_0}, \\ P[\overline{+}] &\simeq \frac{(1-q)\rho^{+-}\rho_1}{2\rho^-}, & P[\overline{+}] &\simeq \frac{q\rho^{+-}\rho_{10}}{4\rho^-\rho_0}. \end{aligned} \quad (\text{A8})$$

Finally, plugging into Eq. (A6) the approximate expressions for the conditional probabilities from Eqs. (A8) and for $P(\overline{+})$ from Eq. (A7) we arrive to

$$\Delta\rho^+|_{\overline{+} \rightarrow +} = \frac{\rho^{+-}}{2N} \left[\rho_0 - q(1-p_o)\frac{\rho_{10}}{2} \right], \quad (\text{A9})$$

where we have used the conservation relations Eqs. (2a) and (2d).

We now calculate the second gain term in Eq. (A1), $\Delta\rho^+|_{\overline{+} \rightarrow +}$, which represents the average change in ρ^+ due to $[\overline{+}] \rightarrow [+]$ transitions, following the same steps as above for the term $\Delta\rho^+|_{\overline{+} \rightarrow +}$. From Eq. (A3) we obtain

$$\begin{aligned} \Delta\rho^+|_{\overline{+} \rightarrow +} &= P(\overline{+}) \sum_{\{\mathcal{N}_1^-\}}^{\mu} M(\{\mathcal{N}_1^-\}, \mu) \frac{1}{\mu} \left\{ \mathcal{N}[\overline{+}] + p_o \mathcal{N}[\overline{+}] + \mathcal{N}[\overline{+}] + p_o \mathcal{N}[\overline{+}] \right\} \frac{1}{N} \\ &= \frac{P(\overline{+})}{\mu N} \left\{ \langle \mathcal{N}[\overline{+}] \rangle + \langle \mathcal{N}[\overline{+}] \rangle + p_o (\langle \mathcal{N}[\overline{+}] \rangle + \langle \mathcal{N}[\overline{+}] \rangle) \right\} \\ &= \frac{P(\overline{+})}{N} \left\{ P[\overline{+}] + P[\overline{+}] + p_o (P[\overline{+}] + P[\overline{+}]) \right\}, \end{aligned}$$

and using the approximations

$$\begin{aligned} P[\overline{+}] &\simeq \frac{(1-q)\rho^{+-}\rho_0}{2\rho^-}, & P[\overline{+}] &\simeq \frac{q\rho^{+-}\rho_{10}}{4\rho^-\rho_1}, \\ P[\overline{+}] &\simeq \frac{(1-q)\rho^{+-}\rho_1}{2\rho^-}, & P[\overline{+}] &\simeq \frac{q\rho^{+-}\rho_{11}}{2\rho^-\rho_1}, \end{aligned} \quad (\text{A10})$$

for the conditional probabilities we arrive to

$$\Delta\rho^+|_{\overline{+} \rightarrow +} = \frac{\rho^{+-}\rho_1}{2N} [1 - q(1-p_o)], \quad (\text{A11})$$

where we have used the conservation relations Eqs. (2a) and (2c).

Adding Eqs. (A9) and (A11) we obtain the following expression for the average gain of a $+$ node in single time step, corresponding to the sum of the first and second terms of Eq. (A1)

$$\frac{d\rho^+}{dt} \Big|_{\rightarrow +} = \frac{1}{1/N} \left[\Delta\rho^+|_{\overline{+} \rightarrow +} + \Delta\rho^+|_{\overline{+} \rightarrow +} \right] \simeq \frac{1}{2} \omega \rho^{+-}, \quad (\text{A12})$$

with

$$\omega \equiv 1 - q(1 - p_o) \left(\rho_1 + \frac{\rho_{10}}{2} \right). \quad (\text{A13})$$

The prefactor ω plays an important role in the dynamics of opinion consensus, by setting the time scale associated to opinion updates, and can be interpreted as an effective probability that a node adopts the opinion of randomly chosen opposite-opinion neighbor. That is, Eq. (A12) for the gain of a $+$ node simply describes the process of selecting a $-$ node i and a $+$ neighbor j , which happens with probability $\rho^{+-}/2$, and then switching i 's opinion with a probability ω that depends on the connection type and disease state of both i and j . This “effective copying probability” ω turns out to be an average copying probability over the entire social network, as shown in section IV.

In order to find the equation for the average loss of a $+$ node in a time step, corresponding to the sum of the third and forth terms of Eq. (A1), we can exploit the symmetry between $+$ and $-$ opinion states and simply interchange signs $+$ and $-$ in Eq. (A12)

$$\left. \frac{d\rho^+}{dt} \right|_{+\rightarrow-} = \frac{1}{1/N} \left[\Delta\rho^+ \Big|_{\overset{+}{0} \rightarrow \overset{-}{0}} + \Delta\rho^+ \Big|_{\overset{+}{1} \rightarrow \overset{-}{1}} \right] \simeq -\frac{1}{2}\omega\rho^{+-}, \quad (\text{A14})$$

where we used $\rho^{-+} = \rho^{+-}$. Finally, adding Eqs. (A12) and (A14) we obtain

$$\frac{d\rho^+}{dt} = 0, \quad (\text{A15})$$

quoted in Eq. (3a) of the main text. Therefore, the fractions of $+$ and $-$ nodes are conserved at all times: $\rho^+(t) = \rho^+(0)$ and $\rho^-(t) = \rho^-(0) = 1 - \rho^+(0)$. Even though the above calculation leads to a very simple result, it serves as an introduction to the methodology used for deriving rate equations for the other fractions ρ^{+-} , ρ_1 and ρ_{10} , as we show next.

Appendix B: Derivation of the rate equation for ρ^{+-}

In analogy to the calculation for ρ^+ in the previous section, the average change of the fraction of $+-$ social links ρ^{+-} in a time step is given by the rate equation

$$\frac{d\rho^{+-}}{dt} = \left. \frac{d\rho^{+-}}{dt} \right|_{-\rightarrow+} + \left. \frac{d\rho^{+-}}{dt} \right|_{+\rightarrow-}, \quad (\text{B1})$$

with

$$\left. \frac{d\rho^{+-}}{dt} \right|_{-\rightarrow+} = \frac{1}{1/N} \left[\Delta\rho^{+-} \Big|_{\overset{-}{0} \rightarrow \overset{+}{0}} + \Delta\rho^{+-} \Big|_{\overset{-}{1} \rightarrow \overset{+}{1}} \right] \quad (\text{B2})$$

$$\left. \frac{d\rho^{+-}}{dt} \right|_{+\rightarrow-} = \frac{1}{1/N} \left[\Delta\rho^{+-} \Big|_{\overset{+}{0} \rightarrow \overset{-}{0}} + \Delta\rho^{+-} \Big|_{\overset{+}{1} \rightarrow \overset{-}{1}} \right] = \left\{ \left. \frac{d\rho^{+-}}{dt} \right|_{-\rightarrow+} \right\}^{-\leftrightarrow+}, \quad (\text{B3})$$

where the symbol $- \iff +$ indicates the interchange of signs $+$ and $-$ in the expression between braces. Equation (B3) means that the symmetry between $+$ and $-$ opinions allows to find the second term in Eq. (B1) by interchanging signs in the first term. To calculate the first term in Eq. (B2) we sum over all four types of interactions of a $\begin{bmatrix} - \\ 0 \end{bmatrix}$ node i with a $\begin{bmatrix} + \\ \mathcal{D} \end{bmatrix}$ neighbor j that lead to the $\begin{bmatrix} - \\ 0 \end{bmatrix} \rightarrow \begin{bmatrix} + \\ 0 \end{bmatrix}$ transition

$$\Delta\rho^{+-}\Big|_{\begin{bmatrix} - \\ 0 \end{bmatrix} \rightarrow \begin{bmatrix} + \\ 0 \end{bmatrix}} = \Delta\rho^{+-}\Big|_{\begin{bmatrix} - \\ 0 \end{bmatrix} \rightarrow \begin{bmatrix} + \\ 0 \end{bmatrix}} + \Delta\rho^{+-}\Big|_{\begin{bmatrix} - \\ 0 \end{bmatrix} \rightarrow \begin{bmatrix} + \\ 0 \end{bmatrix}} + \Delta\rho^{+-}\Big|_{\begin{bmatrix} - \\ 0 \end{bmatrix} \rightarrow \begin{bmatrix} + \\ 0 \end{bmatrix}} + \Delta\rho^{+-}\Big|_{\begin{bmatrix} - \\ 0 \end{bmatrix} \rightarrow \begin{bmatrix} + \\ 0 \end{bmatrix}}. \quad (\text{B4})$$

As explained in the previous section, the probabilities of interactions $\begin{bmatrix} - \\ 0 \end{bmatrix}$ and $\begin{bmatrix} - \\ 0 \end{bmatrix}$ are given by the respective fractions $\mathcal{N}[\begin{bmatrix} - \\ 0 \end{bmatrix}]/\mu$ and $\mathcal{N}[\begin{bmatrix} - \\ 0 \end{bmatrix}]/\mu$ of each type of neighbor. The change in the number of $+-$ social links after node i switches opinion is given by the expression $\mu - 2(\mathcal{N}[\begin{bmatrix} - \\ 0 \end{bmatrix}] + \mathcal{N}[\begin{bmatrix} - \\ 0 \end{bmatrix}] + \mathcal{N}[\begin{bmatrix} - \\ 0 \end{bmatrix}] + \mathcal{N}[\begin{bmatrix} - \\ 0 \end{bmatrix}])$, which takes into account the specific configuration of links and neighbors connected to i , as depicted in Fig. 10. We obtain

$$\begin{aligned} \Delta\rho^{+-}\Big|_{\begin{bmatrix} - \\ 0 \end{bmatrix} \rightarrow \begin{bmatrix} + \\ 0 \end{bmatrix}} &= P\left(\begin{bmatrix} - \\ 0 \end{bmatrix}\right) \sum_{\{\mathcal{N}_0^-\}}^{\mu} \frac{M(\{\mathcal{N}_0^-\}, \mu)}{\mu} (\mathcal{N}[\begin{bmatrix} - \\ 0 \end{bmatrix}] + \mathcal{N}[\begin{bmatrix} - \\ 0 \end{bmatrix}] + \mathcal{N}[\begin{bmatrix} - \\ 0 \end{bmatrix}] + p_o \mathcal{N}[\begin{bmatrix} - \\ 0 \end{bmatrix}]) \\ &\times \frac{[\mu - 2(\mathcal{N}[\begin{bmatrix} - \\ 0 \end{bmatrix}] + \mathcal{N}[\begin{bmatrix} - \\ 0 \end{bmatrix}] + \mathcal{N}[\begin{bmatrix} - \\ 0 \end{bmatrix}] + \mathcal{N}[\begin{bmatrix} - \\ 0 \end{bmatrix}])]}{\mu N/2} \end{aligned} \quad (\text{B5})$$

$$\begin{aligned} &= \frac{2P\left(\begin{bmatrix} - \\ 0 \end{bmatrix}\right)}{\mu^2 N} \left\{ \mu \left[\langle \mathcal{N}[\begin{bmatrix} - \\ 0 \end{bmatrix}] \rangle + \langle \mathcal{N}[\begin{bmatrix} - \\ 0 \end{bmatrix}] \rangle + \langle \mathcal{N}[\begin{bmatrix} - \\ 0 \end{bmatrix}] \rangle + p_o \langle \mathcal{N}[\begin{bmatrix} - \\ 0 \end{bmatrix}] \rangle \right] \right. \\ &- 2 \left[\langle \mathcal{N}[\begin{bmatrix} - \\ 0 \end{bmatrix}]^2 \rangle + \langle \mathcal{N}[\begin{bmatrix} - \\ 0 \end{bmatrix}]^2 \rangle + \langle \mathcal{N}[\begin{bmatrix} - \\ 0 \end{bmatrix}]^2 \rangle + p_o \langle \mathcal{N}[\begin{bmatrix} - \\ 0 \end{bmatrix}]^2 \rangle \right. \\ &+ 2(\langle \mathcal{N}[\begin{bmatrix} - \\ 0 \end{bmatrix}] \mathcal{N}[\begin{bmatrix} - \\ 0 \end{bmatrix}] \rangle + \langle \mathcal{N}[\begin{bmatrix} - \\ 0 \end{bmatrix}] \mathcal{N}[\begin{bmatrix} - \\ 0 \end{bmatrix}] \rangle + \langle \mathcal{N}[\begin{bmatrix} - \\ 0 \end{bmatrix}] \mathcal{N}[\begin{bmatrix} - \\ 0 \end{bmatrix}] \rangle) \\ &\left. \left. + (1 + p_o)(\langle \mathcal{N}[\begin{bmatrix} - \\ 0 \end{bmatrix}] \mathcal{N}[\begin{bmatrix} - \\ 0 \end{bmatrix}] \rangle + \langle \mathcal{N}[\begin{bmatrix} - \\ 0 \end{bmatrix}] \mathcal{N}[\begin{bmatrix} - \\ 0 \end{bmatrix}] \rangle + \langle \mathcal{N}[\begin{bmatrix} - \\ 0 \end{bmatrix}] \mathcal{N}[\begin{bmatrix} - \\ 0 \end{bmatrix}] \rangle) \right] \right\}, \quad (\text{B6}) \end{aligned}$$

where the first and second moments of $M(\{\mathcal{N}_0^-\}, \mu)$ are

$$\begin{aligned} \langle \mathcal{N}[\begin{bmatrix} - \\ \mathcal{D}_i \mathcal{D}_j \end{bmatrix}] \rangle &= \mu P[\begin{bmatrix} - \\ \mathcal{D}_i \mathcal{D}_j \end{bmatrix}], \\ \langle \mathcal{N}[\begin{bmatrix} - \\ \mathcal{D}_i \mathcal{D}_j \end{bmatrix}] \rangle &= \mu P[\begin{bmatrix} - \\ \mathcal{D}_i \mathcal{D}_j \end{bmatrix}], \\ \langle \mathcal{N}[\begin{bmatrix} - \\ \mathcal{D}_i \mathcal{D}_j \end{bmatrix}]^2 \rangle &= \mu P[\begin{bmatrix} - \\ \mathcal{D}_i \mathcal{D}_j \end{bmatrix}] + \mu(\mu - 1) P[\begin{bmatrix} - \\ \mathcal{D}_i \mathcal{D}_j \end{bmatrix}]^2, \\ \langle \mathcal{N}[\begin{bmatrix} - \\ \mathcal{D}_i \mathcal{D}_j \end{bmatrix}]^2 \rangle &= \mu P[\begin{bmatrix} - \\ \mathcal{D}_i \mathcal{D}_j \end{bmatrix}] + \mu(\mu - 1) P[\begin{bmatrix} - \\ \mathcal{D}_i \mathcal{D}_j \end{bmatrix}]^2, \\ \langle \mathcal{N}[\begin{bmatrix} - \\ \mathcal{D}_i \mathcal{D}_j \end{bmatrix}] \mathcal{N}[\begin{bmatrix} - \\ \mathcal{D}_i \mathcal{D}_j' \end{bmatrix}] \rangle &= \mu(\mu - 1) P[\begin{bmatrix} - \\ \mathcal{D}_i \mathcal{D}_j \end{bmatrix}] P[\begin{bmatrix} - \\ \mathcal{D}_i \mathcal{D}_j' \end{bmatrix}], \\ \langle \mathcal{N}[\begin{bmatrix} - \\ \mathcal{D}_i \mathcal{D}_j \end{bmatrix}] \mathcal{N}[\begin{bmatrix} - \\ \mathcal{D}_i \mathcal{D}_j' \end{bmatrix}] \rangle &= \mu(\mu - 1) P[\begin{bmatrix} - \\ \mathcal{D}_i \mathcal{D}_j \end{bmatrix}] P[\begin{bmatrix} - \\ \mathcal{D}_i \mathcal{D}_j' \end{bmatrix}], \\ \langle \mathcal{N}[\begin{bmatrix} - \\ \mathcal{D}_i \mathcal{D}_j \end{bmatrix}] \mathcal{N}[\begin{bmatrix} - \\ \mathcal{D}_i \mathcal{D}_j' \end{bmatrix}] \rangle &= \mu(\mu - 1) P[\begin{bmatrix} - \\ \mathcal{D}_i \mathcal{D}_j \end{bmatrix}] P[\begin{bmatrix} - \\ \mathcal{D}_i \mathcal{D}_j' \end{bmatrix}]. \end{aligned} \quad (\text{B7})$$

Here $\mathcal{D}_i = 1, 0$ and $\mathcal{D}_j = 1, 0$ are the disease states of nodes i and j , respectively. Replacing the expressions for the moments from Eqs. (B7) in Eq. (B6) and regrouping terms we obtain

$$\begin{aligned} \Delta\rho^{+-}\big|_{\bar{0} \rightarrow \bar{0}} = & \frac{2P(\bar{0})}{\mu N} \left\{ (\mu - 2) \left[P[\bar{0}\bar{0}] + P[\bar{0}\bar{0}] + P[\bar{0}\bar{1}] + p_o P[\bar{0}\bar{1}] \right] \right. \\ & - 2(\mu - 1) \left[(P[\bar{0}\bar{0}] + P[\bar{0}\bar{0}] + P[\bar{0}\bar{1}])^2 + p_o P[\bar{0}\bar{1}]^2 \right. \\ & \left. \left. + (1 + p_o) P[\bar{0}\bar{1}] (P[\bar{0}\bar{0}] + P[\bar{0}\bar{0}] + P[\bar{0}\bar{1}]) \right] \right\}. \end{aligned} \quad (\text{B8})$$

Plugging the expressions for the probabilities $P[\bar{0}\bar{0}]$ and $P[\bar{0}\bar{0}]$ from Eq. (A8) into Eq. (B8), and after doing some algebra we finally obtain

$$\Delta\rho^{+-}\big|_{\bar{0} \rightarrow \bar{0}} = \frac{\rho^{+-}}{\mu N} \left\{ (\mu - 2) \left[(1 - q)\rho_0 + q \left(\rho_{00} + p_o \frac{\rho_{10}}{2} \right) \right] - (\mu - 1) \frac{\rho^{+-}}{\rho^-} \left[\rho_0 - (1 - p_o)q \frac{\rho_{10}}{2} \right] \right\}. \quad (\text{B9})$$

We now follow an approach similar to the one above for $\Delta\rho^{+-}\big|_{\bar{0} \rightarrow \bar{0}}$ and calculate the second term of Eq. (B2) as

$$\begin{aligned} \Delta\rho^{+-}\big|_{\bar{1} \rightarrow \bar{1}} &= P(\bar{1}) \sum_{\{\mathcal{N}_1^-\}}^{\mu} \frac{M(\{\mathcal{N}_1^-\}, \mu)}{\mu} [\mathcal{N}[\bar{1}\bar{0}] + \mathcal{N}[\bar{1}\bar{1}] + p_o(\mathcal{N}[\bar{1}\bar{0}] + \mathcal{N}[\bar{1}\bar{1}])] \\ &\times \frac{[\mu - 2(\mathcal{N}[\bar{1}\bar{0}] + \mathcal{N}[\bar{1}\bar{0}] + \mathcal{N}[\bar{1}\bar{1}] + \mathcal{N}[\bar{1}\bar{1}])]}{\mu N/2} \\ &= \frac{2P(\bar{1})}{\mu^2 N} \left\{ \mu \left[\langle \mathcal{N}[\bar{1}\bar{0}] \rangle + \langle \mathcal{N}[\bar{1}\bar{1}] \rangle + p_o(\langle \mathcal{N}[\bar{1}\bar{0}] \rangle + \langle \mathcal{N}[\bar{1}\bar{1}] \rangle) \right] \right. \\ &- 2 \left[\langle \mathcal{N}[\bar{1}\bar{0}]^2 \rangle + \langle \mathcal{N}[\bar{1}\bar{1}]^2 \rangle + p_o(\langle \mathcal{N}[\bar{1}\bar{0}]^2 \rangle + \langle \mathcal{N}[\bar{1}\bar{1}]^2 \rangle) + 2\langle \mathcal{N}[\bar{1}\bar{0}] \mathcal{N}[\bar{1}\bar{1}] \rangle \right. \\ &+ (1 + p_o)(\langle \mathcal{N}[\bar{1}\bar{0}] \mathcal{N}[\bar{1}\bar{0}] \rangle + \langle \mathcal{N}[\bar{1}\bar{0}] \mathcal{N}[\bar{1}\bar{1}] \rangle + \langle \mathcal{N}[\bar{1}\bar{0}] \mathcal{N}[\bar{1}\bar{1}] \rangle + \langle \mathcal{N}[\bar{1}\bar{1}] \mathcal{N}[\bar{1}\bar{1}] \rangle) \\ &\left. \left. + 2p_o \langle \mathcal{N}[\bar{1}\bar{0}] \mathcal{N}[\bar{1}\bar{1}] \rangle \right] \right\} \\ &= \frac{2P(\bar{1})}{\mu N} \left\{ (\mu - 2) \left[P[\bar{1}\bar{0}] + P[\bar{1}\bar{1}] + p_o(P[\bar{1}\bar{0}] + P[\bar{1}\bar{1}]) \right] \right. \\ &- 2(\mu - 1) \left[(P[\bar{1}\bar{0}] + P[\bar{1}\bar{1}])^2 + p_o(P[\bar{1}\bar{0}] + P[\bar{1}\bar{1}])^2 + \right. \\ &\left. \left. + (1 + p_o)(P[\bar{1}\bar{0}] + P[\bar{1}\bar{1}]) (P[\bar{1}\bar{0}] + P[\bar{1}\bar{1}]) \right] \right\}, \end{aligned} \quad (\text{B10})$$

where we have used the moments from Eqs. (B7). After substituting expressions (A10) for the probabilities $P[\bar{1}\bar{0}]$ and $P[\bar{1}\bar{0}]$ we arrive to

$$\Delta\rho^{+-}\big|_{\bar{1} \rightarrow \bar{1}} = \frac{\rho^{+-}}{\mu N} \left\{ (\mu - 2) \left[(1 - q)\rho_1 + q p_o \left(\rho_{11} + \frac{\rho_{10}}{2} \right) \right] - (\mu - 1) \frac{\rho^{+-}\rho_1}{\rho^-} [1 - (1 - p_o)q] \right\}. \quad (\text{B11})$$

By adding Eqs. (B9) and (B11) we obtain the following expression for the change in ρ^{+-} due to $- \rightarrow +$ transitions

$$\left. \frac{d\rho^{+-}}{dt} \right|_{- \rightarrow +} = \frac{\omega\rho^{+-}}{\mu} \left[\mu - 2 - (\mu - 1) \frac{\rho^{+-}}{\rho^-} \right]. \quad (\text{B12})$$

Then, by interchanging signs $+$ and $-$ in Eq. (B12) we obtain the change in ρ^+ due to $+$ \rightarrow $-$ transitions

$$\left. \frac{d\rho^{+-}}{dt} \right|_{+ \rightarrow -} = \frac{\omega\rho^{+-}}{\mu} \left[\mu - 2 - (\mu - 1) \frac{\rho^{+-}}{\rho^+} \right]. \quad (\text{B13})$$

Finally, adding Eqs. (B12) and (B13) we arrive to the following rate equation for ρ^{+-} quoted in Eq. (3b) of the main text

$$\frac{d\rho^{+-}}{dt} = \frac{2\omega\rho^{+-}}{\mu} \left[(\mu - 1) \left(1 - \frac{\rho^{+-}}{2\rho^+\rho^-} \right) - 1 \right].$$

Appendix C: Derivation of the rate equation for ρ_1

The average change of the fraction of infected nodes ρ_1 in a single time step can be written as

$$\frac{d\rho_1}{dt} = \frac{1}{1/N} \left[\Delta\rho_1 \Big|_{+ \rightarrow +} + \Delta\rho_1 \Big|_{+ \rightarrow -} + \Delta\rho_1 \Big|_{- \rightarrow +} + \Delta\rho_1 \Big|_{- \rightarrow -} \right], \quad (\text{C1})$$

where each term represents a different transition corresponding to a disease update on the contact layer. The first term of Eq. (C1) corresponds to the recovery of a $\begin{bmatrix} + \\ 1 \end{bmatrix}$ node, and can be estimated as

$$\Delta\rho_1 \Big|_{+ \rightarrow +} = -P \left(\begin{bmatrix} + \\ 1 \end{bmatrix} \right) (1 - \beta) \frac{1}{N} \simeq -\frac{(1 - \beta)}{N} \rho^+ \rho_1. \quad (\text{C2})$$

That is, with probability $P \left(\begin{bmatrix} + \\ 1 \end{bmatrix} \right) \simeq \rho^+ \rho_1$ a $\begin{bmatrix} + \\ 1 \end{bmatrix}$ node is picked at random, and then recovers with probability $1 - \beta$, decreasing ρ_1 in $1/N$. The second term corresponds to the infection of a $\begin{bmatrix} + \\ 0 \end{bmatrix}$ node, while the last two terms are equivalent to the first two, but where a node with opinion $-$ is recovered and infected, respectively. By the symmetry of $+$ and $-$ opinions, the last two terms are obtained by interchanging signs $+$ and $-$ in the first two.

We now find an approximate expression for the second term of Eq. (C1). A susceptible node j in state $\begin{bmatrix} + \\ 0 \end{bmatrix}$ can be infected by a sick neighbor i with $+$ or $-$ opinion and connected

to j by a contact link or by both a social and a contact link. Thus, four possible contact interactions lead to the $\begin{bmatrix} + \\ 0 \end{bmatrix} \rightarrow \begin{bmatrix} + \\ 1 \end{bmatrix}$ transition:

$$\Delta\rho_1\Big|_{\begin{smallmatrix} + \\ 0 \end{smallmatrix} \rightarrow \begin{smallmatrix} + \\ 1 \end{smallmatrix}} = \Delta\rho_1\Big|_{\begin{smallmatrix} ++ \\ 10 \end{smallmatrix} \rightarrow \begin{smallmatrix} ++ \\ 11 \end{smallmatrix}} + \Delta\rho_1\Big|_{\begin{smallmatrix} ++ \\ 10 \end{smallmatrix} \rightarrow \begin{smallmatrix} +- \\ 11 \end{smallmatrix}} + \Delta\rho_1\Big|_{\begin{smallmatrix} +- \\ 10 \end{smallmatrix} \rightarrow \begin{smallmatrix} +- \\ 11 \end{smallmatrix}} + \Delta\rho_1\Big|_{\begin{smallmatrix} +- \\ 10 \end{smallmatrix} \rightarrow \begin{smallmatrix} -- \\ 11 \end{smallmatrix}}. \quad (\text{C3})$$

The symbol $\begin{bmatrix} \mathcal{O} \\ 1 \end{bmatrix}$ represents a contact interaction between node i in state $\begin{bmatrix} \mathcal{O} \\ 1 \end{bmatrix}$ ($\mathcal{O} = +, -$) and node j in state $\begin{bmatrix} + \\ 0 \end{bmatrix}$. The state that changes in the interaction is now displayed on the right-hand side of the symbol, instead on the left-hand side as for the case of the social interactions described in the previous sections. This is because the chosen neighbor j of i changes state in the CP, while in the VM is node i who changes state. Taking into account the events and their associated probabilities that lead to each of the four interactions described above, we can write Eq. (C3) as

$$\begin{aligned} \Delta\rho_1\Big|_{\begin{smallmatrix} + \\ 0 \end{smallmatrix} \rightarrow \begin{smallmatrix} + \\ 1 \end{smallmatrix}} &= P\left(\begin{smallmatrix} + \\ 1 \end{smallmatrix}\right) \sum_{\{\mathcal{N}_1^+\}}^{\mu} M(\{\mathcal{N}_1^+\}, \mu) \frac{\beta}{\mu} (\mathcal{N}[\begin{smallmatrix} ++ \\ 10 \end{smallmatrix}] + \mathcal{N}[\begin{smallmatrix} +- \\ 10 \end{smallmatrix}]) \frac{1}{N} \\ &+ P\left(\begin{smallmatrix} - \\ 1 \end{smallmatrix}\right) \sum_{\{\mathcal{N}_1^-\}}^{\mu} M(\{\mathcal{N}_1^-\}, \mu) \frac{\beta}{\mu} (\mathcal{N}[\begin{smallmatrix} +- \\ 10 \end{smallmatrix}] + p_d \mathcal{N}[\begin{smallmatrix} -- \\ 10 \end{smallmatrix}]) \frac{1}{N}. \end{aligned} \quad (\text{C4})$$

The first and third terms of Eq. (C4) correspond to selecting an $\begin{bmatrix} \mathcal{O} \\ 1 \end{bmatrix}$ node i and a contact neighbor j with state $\begin{bmatrix} + \\ 0 \end{bmatrix}$ at random, which happens with probability $P\left(\begin{smallmatrix} \mathcal{O} \\ 1 \end{smallmatrix}\right) \mathcal{N}[\begin{smallmatrix} \mathcal{O}+ \\ 10 \end{smallmatrix}]/\mu$, and then i infecting j with probability β , given that they are not connected by a social link. The second and fourth terms are similar to the first and second terms, respectively, but selecting a social/contact neighbor j . As both types of links are present in this case, i infects j with probability βp_d when both nodes have different opinions (fourth term). In all cases ρ_1 changes by $1/N$. Performing the sums of Eq. (C4) we obtain

$$\Delta\rho_1\Big|_{\begin{smallmatrix} + \\ 0 \end{smallmatrix} \rightarrow \begin{smallmatrix} + \\ 1 \end{smallmatrix}} = \frac{\beta}{\mu N} \left[P\left(\begin{smallmatrix} + \\ 1 \end{smallmatrix}\right) (\langle \mathcal{N}[\begin{smallmatrix} ++ \\ 10 \end{smallmatrix}] \rangle + \langle \mathcal{N}[\begin{smallmatrix} +- \\ 10 \end{smallmatrix}] \rangle) + P\left(\begin{smallmatrix} - \\ 1 \end{smallmatrix}\right) (\langle \mathcal{N}[\begin{smallmatrix} +- \\ 10 \end{smallmatrix}] \rangle + p_d \langle \mathcal{N}[\begin{smallmatrix} -- \\ 10 \end{smallmatrix}] \rangle) \right]. \quad (\text{C5})$$

Replacing the expressions for the first moments $\langle \mathcal{N}[\begin{smallmatrix} \mathcal{O}+ \\ 10 \end{smallmatrix}] \rangle = \mu P[\begin{smallmatrix} \mathcal{O}+ \\ 10 \end{smallmatrix}]$ and $\langle \mathcal{N}[\begin{smallmatrix} \mathcal{O}- \\ 10 \end{smallmatrix}] \rangle = \mu P[\begin{smallmatrix} \mathcal{O}- \\ 10 \end{smallmatrix}]$ in Eq. (C5), and using the following expressions for the conditional probabilities

$$P[\begin{smallmatrix} ++ \\ 10 \end{smallmatrix}] \simeq \frac{(1-q)\rho^+\rho_{10}}{2\rho_1}, \quad P[\begin{smallmatrix} +- \\ 10 \end{smallmatrix}] \simeq \frac{q\rho^{++}\rho_{10}}{2\rho^+\rho_1}, \quad (\text{C6})$$

$$P[\begin{smallmatrix} -+ \\ 10 \end{smallmatrix}] \simeq \frac{(1-q)\rho^+\rho_{10}}{2\rho_1}, \quad P[\begin{smallmatrix} -- \\ 10 \end{smallmatrix}] \simeq \frac{q\rho^{+-}\rho_{10}}{4\rho^-\rho_1}, \quad (\text{C7})$$

we finally arrive to

$$\Delta\rho_1\Big|_{\begin{smallmatrix} + \\ 0 \end{smallmatrix} \rightarrow \begin{smallmatrix} + \\ 1 \end{smallmatrix}} \simeq \frac{\beta\rho_{10}}{2N} \left[\rho^+ - \frac{q}{2}(1-p_d)\rho^{+-} \right], \quad (\text{C8})$$

where we have used the conservation relations from Eqs. (1a) and (1c).

Now that we estimated the first two terms of Eq. (C1), the last two terms are obtained by interchanging signs $+$ and $-$ in Eqs. (C2) and (C8):

$$\Delta\rho_1|_{\bar{1}\rightarrow\bar{0}} \simeq -\frac{(1-\beta)}{N}\rho^-\rho_1, \quad (\text{C9})$$

$$\Delta\rho_1|_{\bar{0}\rightarrow\bar{1}} \simeq \frac{\beta\rho_{10}}{2N}\left[\rho^- - \frac{q}{2}(1-p_d)\rho^{+-}\right]. \quad (\text{C10})$$

Adding Eqs. (C2), (C8), (C9) and (C10), the rate equation (C1) for ρ_1 becomes

$$\frac{d\rho_1}{dt} \simeq \frac{\gamma\beta\rho_{10}}{2} - (1-\beta)\rho_1, \quad (\text{C11})$$

with

$$\gamma \equiv 1 - q(1-p_d)\rho^{+-}, \quad (\text{C12})$$

as quoted in Eqs. (5a) and (6) of the main text.

Appendix D: Derivation of the rate equation for ρ_{10}

The average change of the fraction of infected-susceptible pairs of nodes ρ_{10} in a single time step can be written as

$$\frac{d\rho_{10}}{dt} = \frac{1}{1/N}\left[\Delta\rho_{10}|_{+ \rightarrow +} + \Delta\rho_{10}|_{+ \rightarrow -}\right] + \frac{1}{1/N}\left[\Delta\rho_{10}|_{- \rightarrow +} + \Delta\rho_{10}|_{- \rightarrow -}\right], \quad (\text{D1})$$

where the first and second terms correspond to the change in ρ_{10} due to the recovery of a $\left[\begin{smallmatrix} + \\ 1 \end{smallmatrix}\right]$ node and the infection of a $\left[\begin{smallmatrix} + \\ 0 \end{smallmatrix}\right]$ node, respectively, while the last two terms are the corresponding recovery and infections events of nodes with $-$ opinion, and are obtained by interchanging the symbols $+$ and $-$ in the first two terms. The recovery term can be calculated as

$$\Delta\rho_{10}|_{+ \rightarrow +} = P\left(\begin{smallmatrix} + \\ 1 \end{smallmatrix}\right)(1-\beta)\sum_{\{\mathcal{N}_1^+\}}^{\mu} M(\{\mathcal{N}_1^+\}, \mu) \frac{[\mu - 2(\mathcal{N}[\begin{smallmatrix} ++ \\ 10 \end{smallmatrix}] + \mathcal{N}[\begin{smallmatrix} +- \\ 10 \end{smallmatrix}] + \mathcal{N}[\begin{smallmatrix} -+ \\ 10 \end{smallmatrix}] + \mathcal{N}[\begin{smallmatrix} -- \\ 10 \end{smallmatrix}])]}{\mu N/2}, \quad (\text{D2})$$

where the expression in square brackets is the change in the number of 10 links connected to a node i in state $\left[\begin{smallmatrix} + \\ 1 \end{smallmatrix}\right]$ when i recovers, given a specific configuration of node types connected to i [see Fig. 11(a)]. The summation in Eq. (D2) leads to the first moments of the multinomial

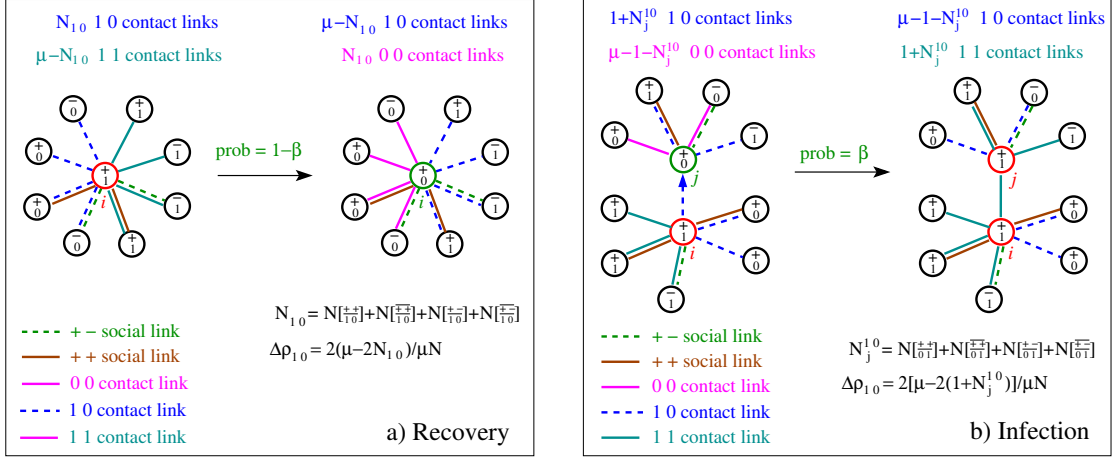


FIG. 11: (Color online) Schematic illustration of two disease updates. (a) Recovery: a node i in state $\begin{bmatrix} + \\ 1 \end{bmatrix}$ recovers with probability $1 - \beta$. (b) Infection: a node i in state $\begin{bmatrix} + \\ 1 \end{bmatrix}$ infects a contact neighbor j in state $\begin{bmatrix} + \\ 0 \end{bmatrix}$ with probability β . The change in the density of 10 contact links is denoted by $\Delta \rho_{10}$.

probability $M(\{\mathcal{N}_1^+\}, \mu)$, with single event probabilities $P[\begin{smallmatrix} ++ \\ 10 \end{smallmatrix}]$ and $P[\begin{smallmatrix} +- \\ 10 \end{smallmatrix}]$ given by Eqs. (C6), and

$$P[\begin{smallmatrix} +- \\ 10 \end{smallmatrix}] \simeq \frac{(1 - q) \rho^- \rho_{10}}{2\rho_1}, \quad P[\begin{smallmatrix} ++ \\ 10 \end{smallmatrix}] \simeq \frac{q \rho^+ \rho_{10}}{4\rho^+ \rho_1}. \quad (\text{D3})$$

Replacing these expressions for the probabilities and using the conservation relations from Eqs. (1a) and (1c) we obtain, after doing some algebra,

$$\Delta \rho_{10} \Big|_{+ \rightarrow +} \simeq \frac{2(1 - \beta) \rho^+}{N} (\rho_1 - \rho_{10}). \quad (\text{D4})$$

We now calculate the second term of Eq. (D1) corresponding to the change in ρ_{10} after the infection of a node with $+$ opinion:

$$\begin{aligned} \Delta \rho_{10} \Big|_{+ \rightarrow +} &= \left[P\left(\begin{smallmatrix} + \\ 1 \end{smallmatrix}\right) \sum_{\{\mathcal{N}_{i,1}^+\}}^{\mu} M(\{\mathcal{N}_{i,1}^+\}, \mu) \frac{\beta}{\mu} (\mathcal{N}_i[\begin{smallmatrix} ++ \\ 10 \end{smallmatrix}] + \mathcal{N}_i[\begin{smallmatrix} +- \\ 10 \end{smallmatrix}]) \right. \\ &\quad \left. + P\left(\begin{smallmatrix} - \\ 1 \end{smallmatrix}\right) \sum_{\{\mathcal{N}_{i,1}^-\}}^{\mu} M(\{\mathcal{N}_{i,1}^-\}, \mu) \frac{\beta}{\mu} (\mathcal{N}_i[\begin{smallmatrix} -+ \\ 10 \end{smallmatrix}] + p_d \mathcal{N}_i[\begin{smallmatrix} -- \\ 10 \end{smallmatrix}]) \right] \\ &\quad \times \sum_{\{\mathcal{N}_{j,0}^+\}}^{\mu-1} M(\{\mathcal{N}_{j,0}^+\}, \mu-1) \frac{[\mu - 2(1 + \mathcal{N}_j[\begin{smallmatrix} ++ \\ 01 \end{smallmatrix}] + \mathcal{N}_j[\begin{smallmatrix} +- \\ 01 \end{smallmatrix}] + \mathcal{N}_j[\begin{smallmatrix} -+ \\ 01 \end{smallmatrix}] + \mathcal{N}_j[\begin{smallmatrix} -- \\ 01 \end{smallmatrix}])}{\mu N/2} \\ &= \mathcal{P} \times \mathcal{C}. \end{aligned} \quad (\text{D5})$$

The term called \mathcal{P} in Eq. (D5) –the two summations inside the square brackets– is the probability that an $\begin{bmatrix} \mathcal{O} \\ 1 \end{bmatrix}$ node i infects a $\begin{bmatrix} + \\ 0 \end{bmatrix}$ neighbor j , and is the same as the one calculated in Eq. (C4) for $\Delta\rho_1|_{\begin{smallmatrix} + \\ 0 \end{smallmatrix} \rightarrow \begin{smallmatrix} + \\ 1 \end{smallmatrix}}$, which is estimated in Eq. (C8) as

$$\mathcal{P} \simeq \frac{\beta\rho_{10}}{2} \left[\rho^+ - \frac{q}{2}(1-p_d)\rho^{+-} \right]. \quad (\text{D6})$$

We notice that the extra $1/N$ prefactor in Eq. (C8) comes from the change in ρ_1 , which for ρ_{10} depends on the neighborhood of node j . The subindex i in the term \mathcal{P} indicates that the infection probability term depends only on node i and its neighborhood [see Fig. 11(b)]. The term called \mathcal{C} corresponding to the summation outside the square brackets expresses the change in ρ_{10} when node j gets infected [see Fig. 11(b)]. Here the subindex j refers to node j and its neighborhood. This term carries the information that the infection on j comes from one of its infected neighbors i , and thus it is known already that at least one of j 's neighbors has disease state $\mathcal{D}_i = 1$. This is taken into account by running the summation on the other $\mu - 1$ unknown neighbors and considering that the number of 10 links connected to j is at least one, which is added to the total number of 10 links inside the parentheses. Using the conditional probabilities

$$P\left[\begin{smallmatrix} ++ \\ 0+ \end{smallmatrix}\right] \simeq \frac{(1-q)\rho^+\rho_{10}}{2\rho_0}, \quad P\left[\begin{smallmatrix} ++ \\ 0+ \end{smallmatrix}\right] \simeq \frac{q\rho^{++}\rho_{10}}{2\rho^+\rho_0}, \quad (\text{D7})$$

$$P\left[\begin{smallmatrix} +- \\ 0+ \end{smallmatrix}\right] \simeq \frac{(1-q)\rho^-\rho_{10}}{2\rho_0}, \quad P\left[\begin{smallmatrix} +- \\ 0+ \end{smallmatrix}\right] \simeq \frac{q\rho^{+-}\rho_{10}}{4\rho^+\rho_0}, \quad (\text{D8})$$

and the conservation relations Eqs. (1b) and (1c), the change term becomes

$$\mathcal{C} \simeq \frac{2}{\mu N} \left[(\mu - 1) \left(1 - \frac{\rho_{10}}{\rho_0} \right) - 1 \right]. \quad (\text{D9})$$

Finally, combining Eqs. (D6) and (D9) for \mathcal{P} and \mathcal{C} we arrive to

$$\Delta\rho_{10}|_{\begin{smallmatrix} + \\ 0 \end{smallmatrix} \rightarrow \begin{smallmatrix} + \\ 1 \end{smallmatrix}} \simeq \frac{\beta\rho_{10}}{\mu N} \left[\rho^+ - \frac{q}{2}(1-p_d)\rho^{+-} \right] \left[(\mu - 1) \left(1 - \frac{\rho_{10}}{\rho_0} \right) - 1 \right]. \quad (\text{D10})$$

Then, adding the recovery and infection terms from Eqs. (D4) and (D10), respectively, we obtain the first two terms of Eq. (D1), while the last two terms are obtained by interchanging symbols $+$ and $-$ in this last expression. Adding these four terms we arrive to the following rate equation for ρ_{10}

$$\frac{d\rho_{10}}{dt} \simeq \frac{\gamma\beta\rho_{10}}{\mu} \left[(\mu - 1) \left(1 - \frac{\rho_{10}}{\rho_0} \right) - 1 \right] + 2(1 - \beta)(\rho_1 - \rho_{10}), \quad (\text{D11})$$

quoted in Eq. (5b) of the main text.

-
- [1] M. E. J. Newman, SIAM Review **45**, 167 (2003).
 - [2] S. Boccaletti, G. Bianconi, R. Criado, C. I. Del Genio, J. Gómez-Gardeñes, M. Romance, I. Sendia-Nadal, Z. Wang, and M. Zanin, Physics Reports **544**, 1 (2014).
 - [3] M. De Domenico, A. Sole-Ribalta, E. Cozzo, M. Kivela, Y. Moreno, M. A. Porter, S. Gomez, and A. Arenas, Physical Review X **3**, 041022 (2013).
 - [4] M. Kivelä, A. Arenas, M. Barthélemy, J. P. Gleeson, Y. Moreno, and M. A. Porter, Journal of Complex Networks **2**, 203 (2014).
 - [5] T. E. Harris, Ann. Prob. **2**, 969 (1974).
 - [6] J. Marro and R. Dickman, *Non-equilibrium Phase Transitions in Lattice Models* (Cambridge University Press, 1999).
 - [7] R. Ferreira and S. Ferreira, European Physical Journal B **86**, 1 (2013).
 - [8] P. Clifford and A. Sudbury, Biometrika **60**, 581 (1973).
 - [9] R. Holley and T. M. Liggett, Ann. Probab. **4**, 195 (1975).
 - [10] T. M. Liggett, *Interacting Particle Systems* (Springer, Berlin ; New York, 2004).
 - [11] C. Granell, S. Gómez, and A. Arenas, Phys. Rev. Lett. **111**, 128701 (2013).
 - [12] C. Granell, S. Gómez, and A. Arenas, Physical Review E **90**, 012808 (2014).
 - [13] L. G. Alvarez-Zuzek, C. E. La Rocca, F. Vazquez, and L. A. Braunstein, PLOS ONE **11**, e0163593 (2016).
 - [14] A. Halu, K. Zhao, A. Baronchelli, and G. Bianconi, Eurphys. Lett. **102**, 16002 (2013).
 - [15] M. Diakonova, M. San Miguel, and V. Eguíluz, Phys. Rev. E **89**, 062818 (2014).
 - [16] M. Diakonova, V. Nicosia, V. Latora, and M. San Miguel, New Journal of Physics **18**, 023010 (2016).
 - [17] R. Parshani, S. V. Buldyrev, and S. Havlin, Phys. Rev. Lett. **105**, 048701 (2010).
 - [18] Y. Hu, B. Kshirim, R. Cohen, and S. Havlin, Phys. Rev. E **84**, 066116 (2011).
 - [19] J. Gao, S. V. Buldyrev, H. E. Stanley, and S. Havlin, Nature Physics **8**, 40 (2012).
 - [20] D. Zhou, A. Bashan, R. Cohen, Y. Berezin, N. Shnerb, and S. Havlin, Phys. Rev. E **90**, 012803 (2014).
 - [21] F. Radicchi, Nature Physics **9**, 2761 (2013).

- [22] F. Radicchi, Phys. Rev. X **4**, 021014 (2014).
- [23] K. Zhao and G. Bianconi, Journal of Statistical Physics **152(6)**, 1069 (2013).
- [24] A. Czaplicka, R. Toral, and M. San Miguel, arXiv:1605.03479 (2016).
- [25] C. Castellano, D. Vilone, and A. Vespignani, Europhys. Lett. **63**, 153 (2003).
- [26] D. Vilone and C. Castellano, Phys. Rev. E **69**, 016109 (2004).
- [27] K. Suchecki, V. M. Eguíluz, and M. San Miguel, Europhys. Lett. **69**, 228 (2005).
- [28] C. Castellano, V. Loreto, A. Barrat, F. Cecconi, and D. Parisi, Phys. Rev. E **71**, 066107 (2005).
- [29] V. Sood and S. Redner, Physical Review Letters **94**, 178701 (2005).
- [30] F. Vazquez and V. M. Eguíluz, New Journal of Physics **10**, 063011 (2008).
- [31] C. Castellano, M. Marsili, and A. Vespignani, Phys. Rev. Lett. **85**, 3536 (2000).
- [32] F. Vazquez and S. Redner, Eurphys. Lett. **78**, 18002 (2007).